Williams DR, Porter J, Yoon G, Guirao A, Hofer H, Chen L, Cox I, Macrae SM. "How far can we extend the limits of human vision?" In: Krueger RR, Applegate RA, Macrae SM, eds. *Wavefront Customized Visual Correction: The Quest for Supervision II*. Thorofare: Slack, Incorporated, 2004: 19-38.

Chapter 3

How Far Can We Extend the Limits of Human Vision?

David R. Williams, PhD; Jason Porter, MS; Geunyoung Yoon, PhD; Antonio Guirao, PhD; Heidi Hofer, PhD; Li Chen, PhD; Ian Cox, PhD; and Scott M. MacRae, MD

Introduction

Methods to correct the optics of the human eye are at least 700 years old. Spectacles have been used to correct defocus at least as early as the 13th century[1,2] and to correct astigmatism since the 19th century.[3] Though it is well established that the eye suffers from many more monochromatic aberrations than defocus and astigmatism-aberrations we will refer to as higher-order aberrations—there has been relatively little work on correcting them until recently. In 1961, Smirnov, an early pioneer in the characterization of the eye's higher-order aberrations, suggested that it would be possible to manufacture customized lenses to compensate for them in individual eyes.[4] Recent developments increase the probability that Smirnov's suggestion may soon be realized. More rapid and accurate instruments for measuring the ocular aberrations are available, most notably the Shack-Hartmann wavefront sensor, first applied to the eye by Liang et al.[5] Moreover, there are new techniques to correct higher-order aberrations. Liang et al showed that a deformable mirror in an adaptive optics system can correct the eye's higher-order aberrations.[6] This study was the first to demonstrate that the correction of higher-order aberrations can lead to supernormal visual performance in normal eyes. Presently, the visual benefits of adaptive optics can only be obtained in the laboratory due to the relatively large size and high cost of conventional deformable mirrors. Alternative wavefront correctors that are less expensive and more compact, such as Microelectromechanical Systems (MEMS) technology and liquid crystal spatial light modulators, offer the exciting possibility of developing new diagnostic tools incorporating adaptive optics that every clinician would ultimately be able to afford. Nevertheless, the success of adaptive optics encourages the implementation of higher-order correction in everyday vision through customized contact lenses, intraocular lenses (IOLs), or laser refractive surgery. Lathing and laser ablative technologies now exist that can create arbitrary surfaces on contact lenses, offering the possibility of truly customized contact lenses. It has also been shown that conventional IOLs do not produce optimal retinal image quality after cataract surgery, and an IOL that is designed to compensate for the corneal aberrations of the eye would yield better visual outcomes.[7] Finally, there is a major ongoing effort to refine laser refractive surgery to correct other defects besides conventional refractive errors.[8-11]

Ultimately, the visual benefit of attempts to correct higher-order aberrations depends on two things. First, it depends on the relative importance of these aberrations in limiting human vision, and second, on the finesse with which these aberrations can be corrected in everyday vision. The emphasis of this chapter is on the first of these issues: How large are the visual benefits that will accrue from correcting higher-order aberrations and under what conditions will they be realized? We review what is known about the fundamental limits on visual acuity and provide theoretical and empirical evidence concerning the visual significance of higher-order aberrations. There are optical, cone mosaic, and neural factors that limit the finest detail we can see, and an understanding of all three is required to appreciate how much vision can be improved by correcting higher-order aberrations in addition to defocus and astigmatism. For example, as we will see later, improving the eye's optics is not always a good thing. Due to the nature of the limits on visual resolution set by the cone mosaic, improving the optical quality of the eye too much can actually lead to a decline in visual performance on some tasks. Before tackling this apparent paradox, however, we need to review some fundamental aspects of the optical quality of the retinal image.

Optical Limits on Vision

An understanding of the limits the eye's optics place on vision requires a succinct description of the optical quality of the eye, independent of neural factors. In this chapter, we will use the modulation transfer function (MTF) to characterize the ability of the eye's optics to create a sharp image on the retina. The MTF characterizes the quality of an optical system, whether it is a camera, a telescope, or the human eye. The curves of Figure 3-1 show the MTFs for eyes at two pupil sizes, 3 and 7.3 millimeters (mm). These curves reveal how faithfully the eye's optics can form an image of sine waves of different spatial frequency. Sine waves describe the variation in intensity across simple patterns of alternating light and dark bars used as visual stimuli. The x-axis of the MTF represents sine waves with spatial frequency varying from low, corresponding to a large angular spacing between adjacent white bars, to high spatial frequency (ie, fine gratings). Though not as familiar to the clinician as Snellen letters, sine wave gratings also produce a response not only from the optics, but also from the photoreceptor mosaic and the neural visual system, and can provide a richer characterization of how well each stage in the visual system performs. Sine waves

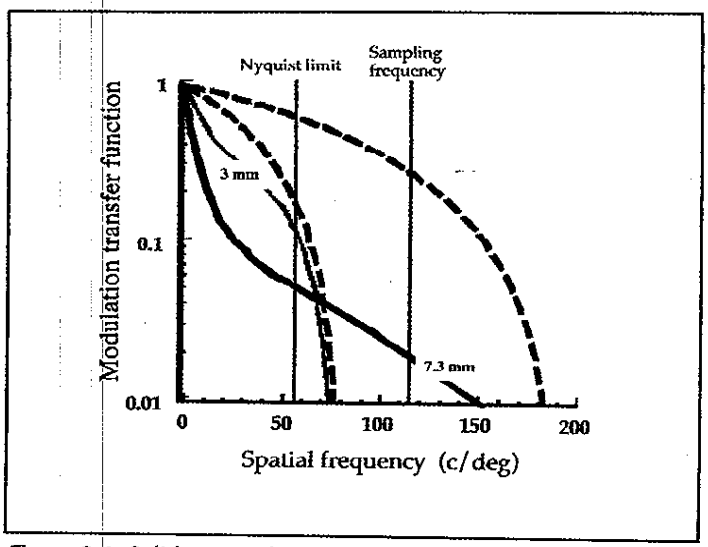

Figure 3-1. Solid curves show MTFs of the eye (averaged across 14 subjects) for two pupil sizes (3 and 7.3 mm diameter) with the correction of astigmatism and defocus, calculated from wavefront sensor measurements of the eye's wave aberration.[12] Dotted curves show the MTF for the same pupil sizes in hypothetical eyes that are free from aberrations and scatter so that the only source of image blur is diffraction. The wavelength was 670 nanometers (nm). The vertical line at 57 cycles/degree (c/deg) corresponds to the Nyquist sampling limit for the average human foveal cone mosaic. The vertical line at 114 c/deg indicates the mosaic sampling frequency.

can be added together to create any visual scene the eye might care to look at. The crucial implication of this fact is that if you know how well the eye images sine waves of different spatial frequency, it is possible to predict the retinal image for any visual scene. Intuitively, the eye's MTF at low spatial frequencies reveals how well the eye images large features in visual scenes, whereas the response to high frequencies tells us how well the eye images fine detail, closer to the limits of visual acuity. The y-axis of the MTF is the modulation transferred by the eye's optics and corresponds to the ratio of the contrast of the sine wave image on the retina to that of the original sine wave pattern viewed by the eye. The more blurring by the eye's optics, the more the modulation transfer departs from a perfect value of 1 and approaches 0.

There are three sources of image blur in the human eye: scatter, diffraction, and aberrations. Even though scatter can degrade vision in older and/or pathological eyes, we will not discuss scatter here because it is generally a minor source of image blur in younger, normal eyes. Diffraction at the eye's pupil is an important source of image blur when the pupil is small, becoming less important with increasing pupil size. The dashed lines in Figure 3-1 show the MTF of eyes that suffer only from diffraction and are free of aberrations. The MTF extends to much higher spatial frequencies (ie, there is less blur from diffraction) for the 7.3 mm pupil than the 3 mm pupil. The highest spatial frequency (expressed in c/deg) that can be imaged on the retina of an aberration-free eye is $\pi p/180\lambda$, where p is the diameter of the pupil and λ the wavelength. Thus, for a 3 mm pupil and a wavelength of 670 nm, the highest spatial frequency that could be viewed in an aberration-free eye is 78 c/deg (190 c/deg for a dilated pupil of 7.3 mm). Blurring by diffraction is unavoidable, quite unlike aberrations, which can be corrected.

The solid curves show the MTFs of normal human eyes for the same 3 and 7.3 mm pupil sizes, but including the blurring effects of the eye's higher-order aberrations as well as diffraction. We have not included blur due to defocus and astigmatism, which conventional spectacles can correct. At low spatial frequencies, the 7.3 mm curve lies below the 3 mm curve because the blurring from aberrations increases strongly with increasing pupil diameter. The central area in the dilated pupil typically has better optical performance than the pupil margin. The aberration-free MTFs lie above the MTFs that include higher-order aberrations, especially for the larger pupil. These results suggest that a rather large increase in retinal image contrast could be achieved by correcting higher-order aberrations when the pupil is large. However, this analysis overestimates the benefit of correcting higher-order aberrations for at least two reasons. First, it does not take account of the limitations on visual acuity imposed by the photoreceptor mosaic and subsequent neural processing, a topic we will address next. Second, this analysis is valid only in monochromatic light, whereas vision normally involves broad band, polychromatic light. As we will see later, in addition to suffering from higher-order monochromatic aberrations, the eye suffers from chromatic aberration that also blurs the retinal image in polychromatic (white light) illumination. Chromatic aberration in an optical system such as the eye causes light rays of different wavelengths to be focused at different positions.

Limits Imposed by the Photoreceptor Mosaic on Vision

The image formed on the retina (or retinal image) is a spatially continuous distribution of light intensity, but the cone mosaic is made of photoreceptors that discretely sample the image. This sampling process results in the loss of information about the retinal image because the brain can never know about the behavior of the retinal image between the sample locations defined by the cone mosaic. The information loss caused by sampling superficially resembles that by optical blurring in that it is high spatial frequencies (ie, fine details in the retinal image) that are affected most. However, there the similarity ends. Optical blurring is a reduction in contrast in the retinal image, whereas sampling does not generally reduce contrast but rather causes errors in the brain's interpretation of the retinal image.

The term used to describe errors due to sampling is *aliasing*. This is because sampling causes high spatial frequencies in the image to masquerade or alias as low spatial frequencies. Figure 3-2A shows this effect for a one-dimensional array of photoreceptors that is sampling two sinusoidal gratings with different spatial frequencies. Notice that the light intensity is identical at each of the sample locations. The cone mosaic is blind to the fact that the retinal images differ between the sample locations defined by the photoreceptors. Since the photoreceptor mosaic does not retain any information that these two images are in fact different, the brain cannot hope to distinguish them. The brain interprets the pattern as the low frequency alternative whether the low or high spatial frequency is in fact present. Figure 3-2B shows aliasing for an array of sample locations taken from an image of the human cone mosaic. When the fundamental spatial frequency of a grating is low, such as for a 30 c/deg grating, the mosaic has an adequate number of samples to represent it and aliasing does not occur.

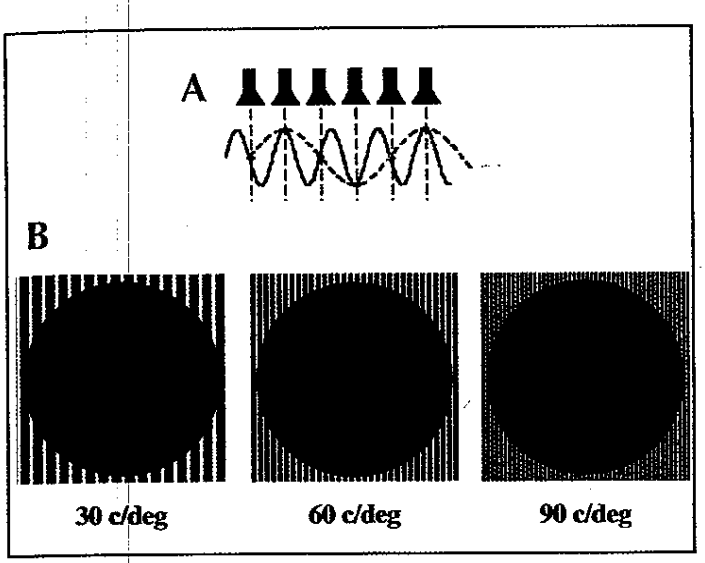

Figure 3-2. (A) Two sinusoidal stimuli sampled by an array of cones. The spatial frequency of one stimulus (solid line) is three times the frequency of the other (dashed line). The cone response is identical for the two patterns, illustrating aliasing, the ambiguity introduced by sampling. (B) Three sinusoidal patterns seen through the same sampling resembling the cone mosaic. After sampling, the high-frequency pattern (90 c/deg) appears as a distorted, low-frequency pattern, though the sampling rate is adequate for the low frequency pattern (30 c/deg). The finest grating pattern that this mosaic can distinctly resolve is set at the Nyquist sampling limit of approximately 60 c/deg.

The 60 c/deg grating represents the highest spatial frequency that can be adequately sampled and represented by this typical photoreceptor mosaic.

However, when the spatial frequency becomes higher, as for the 90 c/deg grating, a low frequency pattern emerges. The irregularity of the low frequency alias is a result of the disorder in the cone mosaic. A 30 c/deg grating has the same spacing between bright bars as the spacing between the horizontal strokes in a 20/20 Snellen letter E. A 60 c/deg grating has a bar spacing corresponding to that of a 20/10 Snellen letter E, and so on.

How can we quantify the limits imposed by the spacing of cones on vision?

Early investigators knew that the finest grating that the eye could resolve required at least one sample for each light and each dark bar of the grating.[3] This simple intuition is captured in modern terms by the sampling theorem, which states that the highest frequency that can be recovered without aliasing from a sampling array is one half the sampling frequency of the array.

The sampling frequency of the array is the reciprocal of the spacing between samples, which in this case is the spacing between rows of cones at the fovea.

Half the sampling frequency is the so-called Nyquist sampling limit. Anatomical and psychophysical estimates of the spacing between rows of foveal cones indicate an average of about 0.51 minutes of arc, which makes the average sampling rate 118 c/deg and the average Nyquist sampling limit half that or about 59 c/deg.

Table 3-1 compares the results of several studies. The conversion between columns in Table 3-1 has been made assuming triangular packing of cones.[14] The Nyquist limit indicates the finest grating patterns that human foveal vision can reasonably expect to resolve in the sense of being able to see the regular stripes of the grating imaged on the retina. Indeed, estimates of the foveal visual acuity for gratings generally agree with the Nyquist sampling limit. In some circumstances, subjects can obtain correct information about, for example, the orientation of a grating at spatial frequencies slightly higher than the Nyquist sampling limit,[15] but the perception of a distinct grating pattern ends at spatial frequencies near the Nyquist sampling limit.

At spatial frequencies above the Nyquist sampling limit, gratings appear more like wavy zebra stripes and appear coarser than the actual gratings on the retina, as shown in Figure 3-3. Williams[14,16] studied these perceptual effects with a laser interferometer, extending earlier reports by Bergmann,[17] Byram,[18] and Campbell and Green,[19] showing conclusively that they result from aliasing by the cone mosaic. Laser interferometry is a method to project gratings, in the form of interference fringes, on the retina that are not blurred by the eye's optics. Gratings with spatial frequencies over 200 c/deg can be imaged on the retina without any appreciable loss of contrast. In the range between 0 and 45 c/deg, interference fringes can be seen as regular stripes across the central foveal region. As the spatial frequency increases toward 60 c/deg, the bars of the fringes can be seen only in a progressively smaller region of the fovea. At about 60 c/deg, the fine, regular bars are lost, and most subjects report the appearance of an annulus of fine wavy lines as shown in Figure 3-3. The annulus corresponds to aliasing by cones just outside the foveal center, which are more widely spaced, and alias at a lower spatial frequency than in the foveal center. As spatial frequency increases, this annulus of wavy lines collapses to a circular patch at a frequency of 90 to 100 c/deg. Subjects describe this patch as resembling a fingerprint or a pattern of zebra stripes. Between 150 and 160 c/deg, the zebra stripe pattern disappears. Due to the sampling limits imposed by the cone mosaic, no matter how much one could improve the eye's optics, one would not expect an increase in visual acuity beyond about 60 c/deg in the average human eye.

Aliasing can potentially distort the appearance of not only grating stimuli but of any visual scene that contains spatial frequencies above the Nyquist sampling limit. For example, sharp edges would be expected to take on a jagged appearance. There are also errors in the color appearance of fine details, referred to as *chromatic aliasing*, caused by the fact that the retina contains three cone submosaics for color vision, each sampling the visual scene even more coarsely than the combined mosaic.[20] Aliasing errors are not generally visible in everyday viewing conditions, partly because the blurring of the retinal image by the eye's optics plays a protective role. This is illustrated in Figure 3-1 which shows that the optical MTF does not allow much contrast in the retinal image at spatial frequencies that exceed the foveal cone Nyquist sampling limit. At the Nyquist sampling limit, the retinal image contrast never exceeds about 10% for any pupil

Table 3-1
Estimates of Human Foveal Cone Sampling

Source	Density (cones/mm²)	Spacing (microns)	Spacing (min of arc)	Nyquist (c/deg)	Acuity (min)
Østerberg (1935)[21]	147 x 10³	2.43	0.50	60	1
Miller (1979)[22]	128 x 10³	2.6	0.54	55.9	1.07
Yuodelis and Hendrikson (1986)[23]	208 x 10³	2.04	0.42	71.4	0.84
Curcio et al. (1987)[24]	162 x 10³	2.57 ± 0.71	0.53 ± 0.15	56.6	1.06
Curcio et al. (1990)[25]	197 x 10³	2.55 ± 0.52	0.53 ± 0.11	56.6	1.06
Williams (1985)[16]	126 x 10³	2.62 ± 0.17	0.54 ± 0.04	55.6	1.08
Williams (1988)[14]	129 x 10³	2.59 ± 0.12	0.54 ± 0.02	55.6	1.08
Average	157 x 10³	2.49	0.51	58.8	1.03

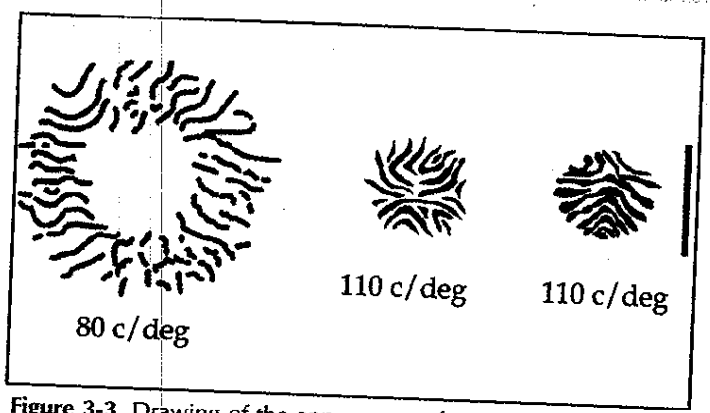

Figure 3-3. Drawing of the appearance of an 80 c/deg and a 110 c/deg (two subjects) interference fringe. Scale bar corresponds to 1 deg of visual angle.[16] The zebra stripe appearance results from aliasing by the cone mosaic.

size, and it is usually far less than this since the contrast in the original scene is usually much less than 100%.

For aliasing to disrupt vision in ordinary scenes, the optical quality of the eye would have to be considerably better than it is.

An indication that this is the case comes from the observation that aliasing errors are not seen in ordinary vision outside the fovea. At an eccentricity of about 4 degrees, the optical quality of the eye is essentially the same as that at the foveal center, yet the Nyquist sampling limit has declined by a factor of about 3. The fact that aliasing is not visible at this eccentricity suggests that the MTF of the eye could be extended by at least a factor of 3 at the fovea without running the risk of incurring aliasing errors there. This realization runs counter to the prevailing view that evolution has matched the optics of the eye and the spacing of foveal cones. Instead, it appears that the optics could afford to be substantially better in the average eye without introducing an important loss of image fidelity due to foveal aliasing. Even in controlled laboratory conditions, it is difficult to produce aliasing effects without the use of interference fringe stimuli. This is true even in extrafoveal vision, which is less protected from aliasing by the eye's optics. Increasing the optical quality of the eye runs a greater risk of causing aliasing outside the fovea. But even outside the fovea, unusually high contrast stimuli are required to cause aliasing and careful attention must be paid to the eye's refractive state.

This is good news for attempts to correct higher-order aberrations in the eye because it suggests that the deleterious effects of sampling and aliasing will not interfere with vision and will not reduce the visual benefit of improving retinal image contrast.

Neural Limits on Vision

Are the postreceptoral retina and the brain equipped to take advantage of the improved optical quality that customized correction can provide? There would be little point in improving the eye's optics if the brain were incapable of resolving the high spatial frequencies restored by a customized correction. Experimentally, this question has been explored by measuring the *contrast sensitivity function* (CSF) with laser interference fringe stimuli.

The CSF is a measure of how sensitive subjects are to gratings of different spatial frequencies. The CSF is determined by finding the threshold contrast at which the subject can detect a sinusoidal grating at each of a number of spatial frequencies. The reciprocal of the threshold is the contrast sensitivity.

At high spatial frequencies, the CSF steadily decreases with spatial frequency, which means that the subject needs higher contrast to detect finer details. This is true even when interference fringes are used to eliminate optical blurring in the eye, as shown in Figure 3-4. This shows that, just as the optics blur the retinal image, the postreceptoral visual system blurs the neural image. The important point is that, despite the neural blur, the nervous system is equipped with the machinery to resolve spatial frequencies as high as the foveal cone Nyquist sampling limit. This makes it quite likely that it can take advantage of improvements in retinal image contrast for spatial frequencies up to the limits set by the photoreceptor mosaic. Indeed, we will show direct empirical evidence for this later.

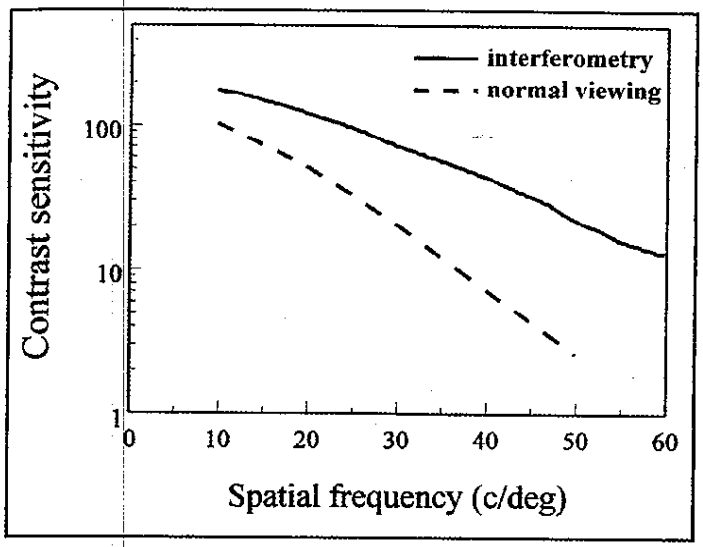

Figure 3-4. CSF measured with interferometry (neural CSF) and CSF for normal viewing conditions for a pupil of 3 mm.[26]

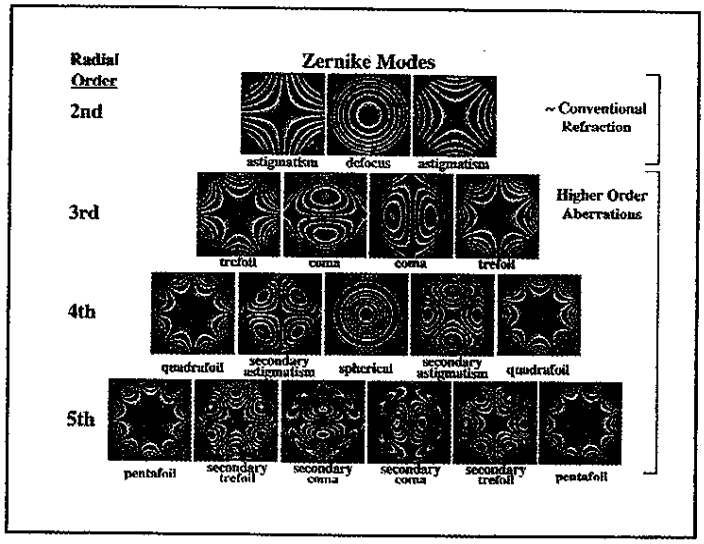

Figure 3-5. Zernike Pyramid. An arbitrary wave aberration can be decomposed into individual Zernike modes. The second-order Zernike modes, which are defocus and two astigmatism terms, can be corrected with a conventional refraction. Higher-order aberrations correspond to Zernike modes of third order and higher.

Visual Benefit of Higher-Order Correction Based on Wave Aberration Measurements

This section describes an analysis of the visual benefit of correcting higher-order aberrations based on measurements of the aberrations found in a large population of eyes. Based on subjective observations of a point source of light, Helmholtz argued that the eye suffered from a host of aberrations that are not found in conventional, man-made optical systems.[27] There have been a number of methods developed to quantify these aberrations.[4,28-33] Liang et al[5] developed a technique based on the Shack-Hartmann principle[34] that provides a rapid, automated, and objective measure of the wave aberration simultaneously at a large number of sample points across the eye's pupil. Using this technique, Liang and Williams provided what is arguably the most complete description to date of the wave aberration of the eye.[12] They measured the eye's aberrations up to 10 radial orders, quantifying the irregular aberrations predicted by Helmholtz and subsequent investigators.[28,29,35]

The wave aberration can be described as the sum of a number of component aberrations such as defocus, astigmatism, coma, spherical aberration, as well as other higher-order aberrations. The wave aberration can be decomposed into these constituent aberrations in much the same way that Fourier analysis can decompose an image into spatial frequency components. For an optical system such as the eye, it is convenient to use Zernike polynomials as the basis functions because of their desirable mathematical properties for circular pupils. In addition, it has been shown using principal components analysis that Zernike polynomials are robust basis functions that adequately capture the majority of aberration variance typically found in human eyes.[36,37] Figure 3-5 shows in two dimensions the first five radial orders (18 Zernike modes) in the Zernike Pyramid of aberrations (excluding piston, tip, and tilt) that are used to compose the eye's wave aberration. Each mode has a value that indicates its magnitude of wavefront error, usually expressed in microns, corresponding to its root mean square (RMS) or standard deviation across the pupil (see Appendix 1).

Defocus is one of the simplest Zernike modes and is the mode that is most closely associated with the spherical refractive error. (Sometimes Zernike defocus does not correspond to the spherical refractive error because higher-order aberrations can also influence the spherical refractive error.)

Clinicians are familiar with defocus in myopia and hyperopia, expressed in diopters (D), which corresponds to the reciprocal of the focal length in meters. In an eye that suffers from defocus alone, the relationship between diopters and the RMS wavefront error is:

$$\text{Diopters (D)} = \frac{4\sqrt{3}Z^0_2}{(\text{pupil radius})^2}$$

where Z^0_2 is the magnitude of the Zernike defocus mode in microns and the pupil radius is in mm. In a normal eye that suffers from defocus and additional aberrations, this equation is only approximately correct, as higher-order aberrations can influence estimates of a patient's best subjective refraction.[38]

From the wave aberration, we can calculate the eye's MTF and phase transfer functions (PTFs), which provide a complete description of retinal image quality. The MTF and PTF can be obtained from the complex autocorrelation of the pupil function, where the pupil function includes the pupil aperture and the wave aberration.[13] Alternately, the point spread function (PSF) captures the same information as the MTF and PTF. The PSF is the Fourier transform of the MTF and PTF. Intuitively, it is the image on the retina of a single point of light, such as the image on the retina when the eye is looking at a star. Figure 3-6 illustrates the PSFs produced by each individual Zernike mode on the retina. We can also calculate any retinal image by the convolution of the object with the PSF. An example of this is shown in Figure 3-7, which illustrates how the retinal image of a visual stimulus sometimes used in psychophysical experiments, called a *binary noise stimulus*, is blurred due to the PSF corresponding to each Zernike term.

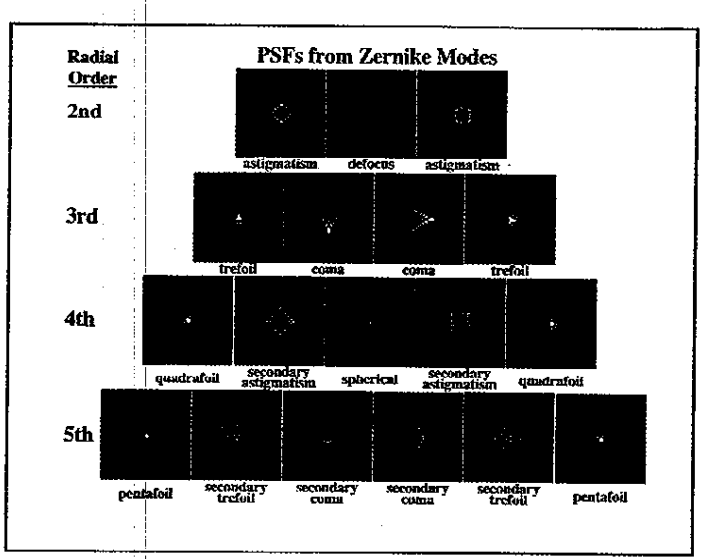

Figure 3-6. Pyramid of PSFs (add-point spread function) obtained from each individual Zernike mode in monochromatic light (550 nm). A PSF is what one would see if looking at a point source of light.

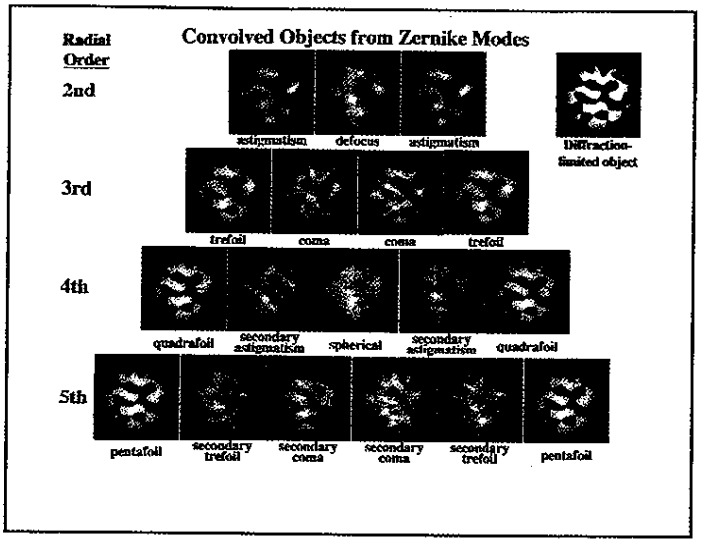

Figure 3-7. Pyramid of retinal images obtained by convolving the PSF produced by each individual Zernike mode (see Figure 3-6) with a binary noise stimulus (the object) in monochromatic light (550 nm). The original object, blurred only by the effect of diffraction, is shown in the top right corner. Aberrations near the center of the pyramid tend to blur the object more than aberrations at the edge.

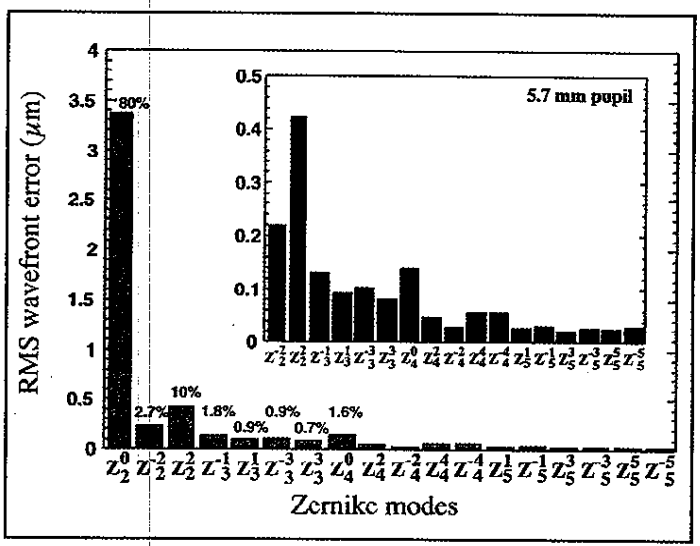

Figure 3-8. Mean absolute RMS values for 18 Zernike modes as measured from a population of 109 normal human subjects for a 5.7 mm pupil. The inset excludes the first Zernike mode corresponding to defocus (Z^0_2) and has an expanded ordinate to illustrate the magnitudes of the higher-order aberrations. Percentages labeled above the first eight modes designate the percent of the variance accounted for by each mode.

The beauty of this is that we can compute from the aberrations, which are defined in the eye's pupil, the impact they will have on the quality of the image formed on the retina. Both diffraction and aberrations are taken into account and it is only light scatter that is ignored, as it is usually small in younger, normal eyes. This computational link between pupil and retina is very valuable because we can use it to deduce the relative importance of different aberrations on image quality. This is critical for deciding which aberrations are worth correcting and which are less important.

An important feature of the eye's wave aberration is that it is a single function that captures all optical defects in both the cornea and the lens. The final retinal image quality depends on the combined effects of the cornea and the lens rather than on the optical quality of each isolated component. For example, in young eyes, the spherical aberration introduced by the cornea is usually reduced by the lens.[39] Other corneal aberrations may also be compensated by the lens in younger subjects.[40,41] These results have important implications for customized correction because they emphasize the necessity to capture the total wave aberration. For example, if the ablation profile in customized laser refractive surgery were computed solely from corneal topography, the final aberrations of the eye could be larger in some cases than before ablation.

For the same amount of RMS wavefront error of each aberration, it is clear from Figure 3-7 that aberrations at the edges of the Zernike pyramid have less subjective blur than those closer to the center of the pyramid.

Population Statistics of the Wave Aberration

A conventional refraction (sphere, cylinder, and axis) typically corrects for only three components of the wave aberration (one defocus and two astigmatic modes). However, if one hopes to achieve a diffraction-limited correction of the eye's optics, a complete description of the wave aberration of normal eyes would require at least 42 individual Zernike modes (corresponding to eighth order) for a large pupil diameter of 7.3 mm.[12] The average magnitudes of the lowest 18 monochromatic aberrations (up to and including fifth order) are presented in Figure 3-8 for 109 normal subjects between the ages of 21 and 65 years (mean age of 41 years) with natural accommodation. Each adult had a spherical refraction between 6 D and -12 D and a refractive astigmatism no larger than -3 D, and no pathological eyes were included in this study.[36] Verifying earlier results reported by Howland and Howland[30] from a smaller subset of eyes, there is a general tendency for the magnitude of the aberrations to decrease with increasing order. The aberration with the largest magnitude is

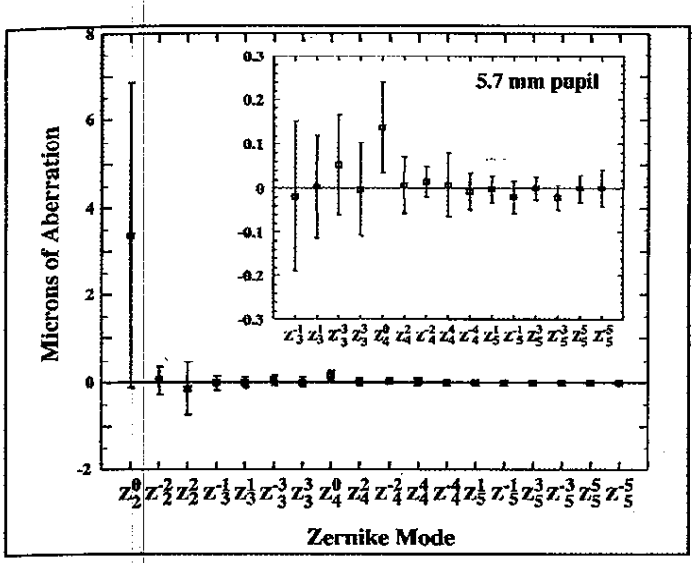

Figure 3-9. Mean values of the first 18 Zernike modes in the population of 109 human subjects for a 5.7 mm pupil. The error bars indicate plus and minus one standard deviation. The inset excludes the first three Zernike modes corresponding to defocus and astigmatism (Z^0_2, Z^{-2}_2, and Z^2_2) and has an expanded ordinate to illustrate the variability of the higher-order aberrations.

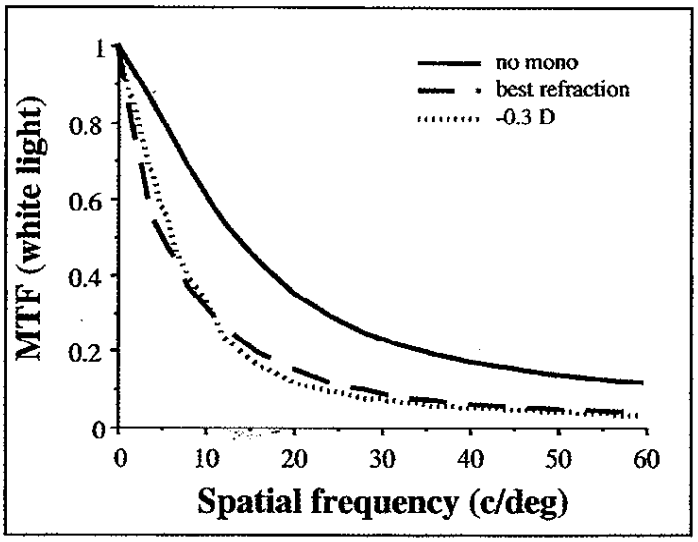

Figure 3-10. White light MTFs (5.7 mm pupil) when correcting all of the eye's monochromatic aberrations (solid line) and when only -0.3 D of defocus are present in the eye (dotted line). The average MTF showing the best correction of defocus and astigmatism from the normal population with higher-order aberrations still present (dashed line) is very similar to the MTF of an eye with only -0.3 D of sphere.

defocus, Z^0_2, followed by the two Zernike modes representing astigmatism, Z^{-2}_2 and Z^2_2. Defocus is expected to be the largest aberration, but it is especially large in this population because the majority of the subjects were patients at a local clinic and tended to be myopic. Higher-order aberrations in this figure correspond to all those beyond the first three. The 15 higher- order aberrations shown here in aggregate account for about two-thirds as much of the variance of the wave aberration as the two modes associated with astigmatism.

In addition to examining the magnitude of each mode, we can also look at the distribution of each Zernike coefficient in the same population. These results, displayed in Figure 3-9, show that each Zernike coefficient, with the exception of spherical aberration, has a mean value that is approximately zero. The mean RMS wavefront error for spherical aberration in this population was 0.138 ± 0.103 μm (5.7 mm pupil).

This indicates that the normal population typically has a tendency toward a slight positive spherical aberration, where the peripheral light rays are focused in front of the central light rays.

Population Statistics of the Visual Benefit of Higher-Order Correction

The magnitude and distribution of monochromatic aberrations in the population of human eyes shown above does not directly provide information on the degree to which higher-order aberrations constructively or destructively interact with each other to improve or degrade retinal image quality. Figure 3-10 compares the white light MTF produced by the eye's higher-order aberrations with that of an eye containing defocus alone. As illustrated in the figure, the average MTF from the normal population for the best correction of defocus and astigmatism (with higher-order aberrations left uncorrected) is nearly identical to the MTF of a hypothetical eye suffering from only -0.3 D of pure defocus, or sphere. The average RMS wavefront error of the higher-order aberrations in the population is equivalent to that produced by -0.3 D of defocus alone, approximately 0.35 microns (μm) (5.7 mm pupil). Of course, these values can be highly variable from patient to patient depending on the amount of higher-order aberration present in each individual eye.

One measure we have developed to inform us directly about the visual improvement resulting from a perfect, theoretical correction of the eye's higher-order aberrations is a quantity we call the *visual benefit*. It is the increase in retinal image contrast at each spatial frequency that would occur if one were to correct all monochromatic aberrations instead of just correcting defocus and astigmatism as one does with a conventional refraction. More specifically, the visual benefit is the ratio of the eye's polychromatic (white light) MTF when all the monochromatic aberrations are corrected to that when only defocus and astigmatism are corrected, as shown in Figure 3-11.

Because customized correction with contact lenses, IOLs, and laser refractive surgery would involve everyday viewing conditions in which the spectra of objects are broad band or polychromatic, we chose to calculate the visual benefit for white light instead of monochromatic light of a single wavelength. The eye suffers from chromatic aberration of two kinds, *axial* and *transverse*. The axial chromatic aberration is the chromatic difference of focus on the optical axis of the eye. Short wavelength (blue) light is brought to a focus nearer to the cornea and lens than the long wavelength (red) light so that only one wavelength in a broad band stimulus can be in focus on the retina at any one time. Wald and Griffin[42] and many other researchers have measured the axial chromatic aberration of the eye. There is almost no variation from observer to observer because all eyes are made of essentially the same materials with the same chromatic dispersion. The total chromatic difference of focus is approximately 2 D over the entire visible spectrum of wavelengths the eye can detect. We have included axial chromatic aberration in the calcu-

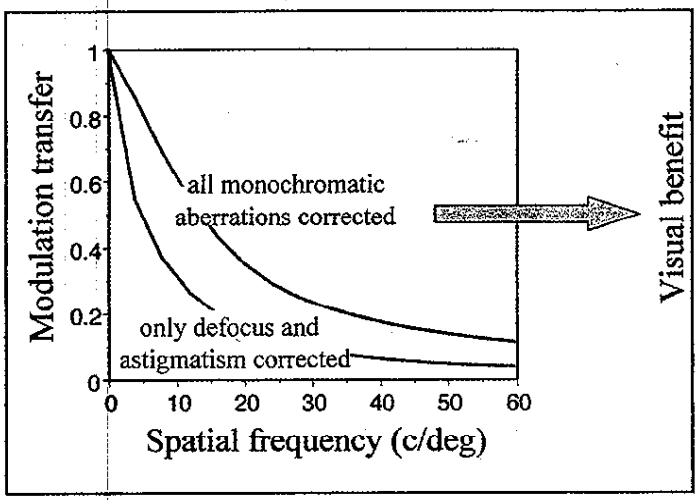

Figure 3-11. The visual benefit is obtained as the ratio between the MTF in white light with no monochromatic aberrations and the eye's MTF in white light with only astigmatism and defocus corrected. The MTF in white light was calculated from the polychromatic PSF determined by integrating the monochromatic PSF affected by the eye's chromatic aberration across the spectrum and weighted with the ocular spectral sensitivity. The baseline MTF corresponding to a conventional correction was calculated by finding the amount of defocus and astigmatism required to maximize the volume of the CSF obtained as the product of the MTF and the neural CSF.

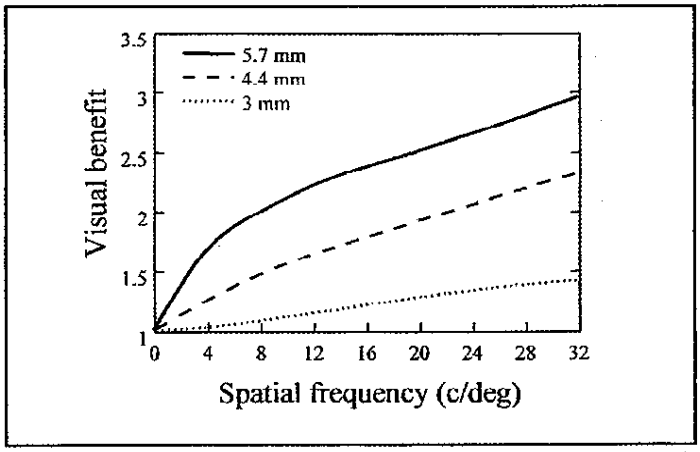

Figure 3-12. Visual benefit at each spatial frequency for three pupil diameters, averaged across a normal population of 109 subjects.

lation of the MTF because, as we will see later, it can have large effects on retinal image quality when one is trying to eliminate all of the aberrations in the eye.

The transverse chromatic aberration (TCA) is the wavelength-dependent displacement of the image position on the retina. In our experience, foveal TCA does not typically reduce retinal image quality very much.

The white light MTF is computed from the polychromatic PSF, which is calculated by first summing the monochromatic PSFs defocused by axial chromatic aberration, shifted by TCA, and weighted by the spectral sensitivity of the eye at each wavelength. The modulus of the Fourier transform of the white light PSF is the white light, or polychromatic, MTF. A visual benefit of 1 corresponds to no benefit of correcting higher-order aberrations. A value of 2 would indicate a two-fold increase in retinal image contrast provided by correcting higher- order aberrations (in addition to defocus and astigmatism). Though the visual benefit is calculated from retinal image quality, the visual benefit is directly applicable to visual performance as assessed with contrast sensitivity measurements. That is, a visual benefit of 2 will lead to a two-fold increase in contrast sensitivity as well as a two-fold increase in retinal image contrast.

Figure 3-12 shows the mean values of the visual benefit across a population of 109 normal subjects, for three different pupil sizes, as a function of the spatial frequency.[43] For a pupil of 3 mm, the visual benefit is modest. For small pupils, diffraction dominates and aberrations beyond defocus and astigmatism are relatively unimportant. A small visual improvement might be realized for the 3 mm pupil at high spatial frequencies (about 1.5 at 32 c/deg). In bright daylight conditions, the natural pupil of most normal eyes is so sufficiently small (~3 mm) that the retinal image would not be greatly affected by aberrations. However, for mid and large pupils, because of the well-known fact that the aberrations grow with increasing pupil size,[12,44] an important visual benefit can be obtained across all spatial frequencies by correcting the monochromatic higher-order aberrations. For example, with a 5.7 mm pupil, the average visual benefit across the population is about 2.5 at 16 c/deg and about 3 at 32 c/deg. This would correspond to a distinct improvement in the sharpness of the retinal image. Thus, for the normal population, the visual benefit of a customized ablation would be greatest in younger patients or individuals who tend to have large pupils, and in situations such as night driving.

Visual benefit is directly applicable to visual performance as assessed with contrast sensitivity measurements. That is, a visual benefit of 2 will lead to a two-fold increase in contrast sensitivity as well as a two-fold increase in retinal image contrast.

What fraction of the population could benefit by correcting the higher-order aberrations? Just as there is large variability in the population in the amount of astigmatism present, so there is variability in the amount of higher-order aberrations. Patients with larger amounts of higher-order aberrations will derive much more visual benefit from higher-order correction than others. The frequency histograms in Figure 3-13 show how much the visual benefit, for a 5.7 mm pupil, varies among eyes in the normal population of 109 normal subjects and in a small cohort of four keratoconic patients. The distributions of visual benefit at spatial frequencies of 16 c/deg and 32 c/deg are shown because they correspond roughly to the highest frequencies that are detectable by normal subjects viewing natural scenes.

Some normal eyes have a visual benefit close to 1 (ie, show almost no benefit of correcting higher-order aberrations). At the other extreme, some normal eyes show a benefit of more than a factor of 5.

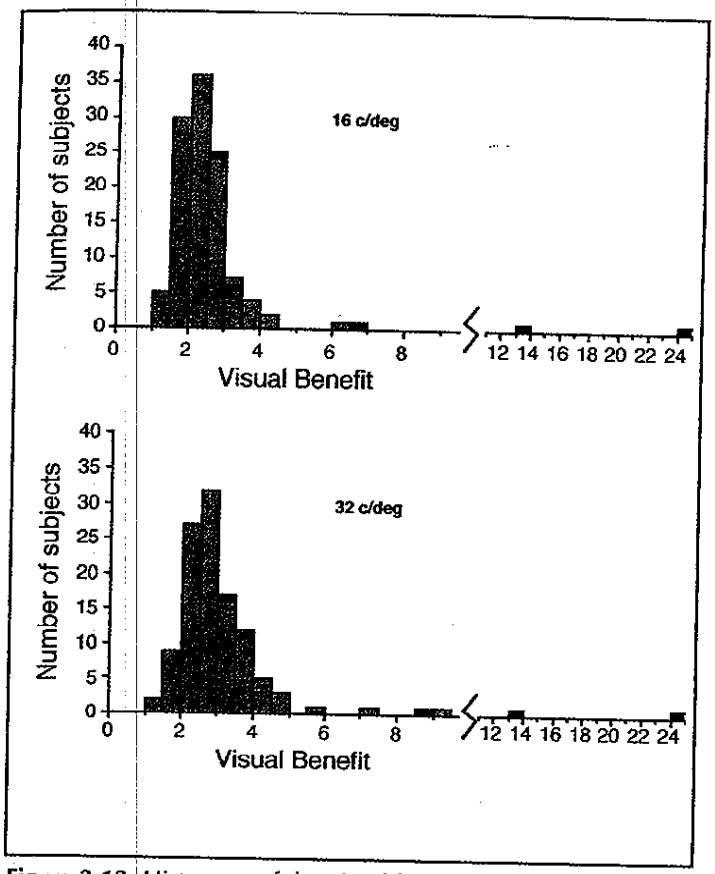

Figure 3-13. Histogram of the visual benefit, at 16 c/deg and 32 c/deg, of correcting higher-order aberrations in white light for a population of 109 normal subjects (green) and a sample of four kerataconic patients (black). Pupil size is 5.7 mm.

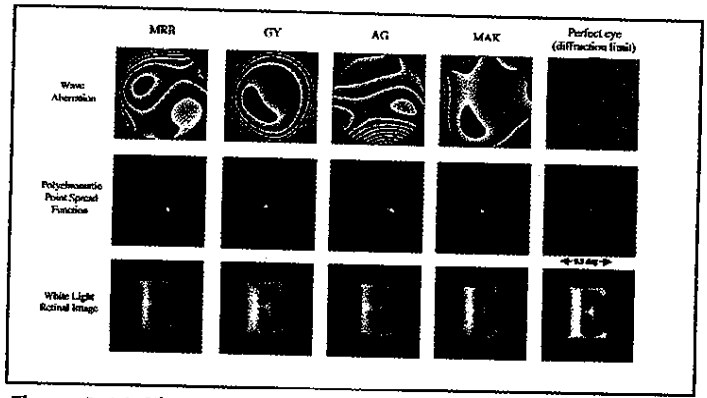

Figure 3-14. The wave aberrations of four typical eyes and a perfect diffraction-limited eye for 5.7 mm pupils are shown at the top. Their corresponding PSFs, computed from the wave aberrations, are shown in the middle row. The bottom row shows the convolution of the PSF with a Snellen letter E, subtending 30 minutes of arc. This shows the retinal image of the letter given the wave aberration measured in each eye. Note the increased blurring in the real eyes compared with the diffraction-limited eye. The calculations were performed assuming white light, axial chromatic aberration in the eye, and that a wavelength of 555 nm was in best focus on the retina.

Editor's note:

The normal population studies by Porter et al[36] demonstrate that some people would have a higher visual benefit from higher-order aberration correction and others would not.[43] We have found this to be true in the clinical excimer laser studies noted later in this book on wavefront-guided customized ablation (Chapters 26 to 31, specifically Chapter 28, Figure 28-7).

S. MacRae, MD

To provide a better indication of the typical visual benefits that subjects would incur with customized correction, Figure 3-14 shows the effect of correcting higher-order aberrations on the retinal image in white light for four subjects over a 5.7 mm pupil. In each case, the PSF computed from the wave aberration is convolved with a letter E subtending 30 minutes of arc, roughly corresponding to the 20/100 line on the Snellen chart. The letters are substantially more blurred than that in the diffraction-limited case, in which there is little or no influence of aberrations. We emphasize that these are the retinal images expected from these eyes and do not necessarily represent the perceptual experience these subjects would have of the retinal images, which is also determined by neural processing.

The visual benefit in the kerataconic patients is typically much larger than that of the normal eyes. One of the subjects of the sample, who is in the early stages of keratoconus, would have a visual benefit similar to the normal population. But the other three show larger benefits than any subject does in the normal population (one of them as high as a factor of 25). Figure 3-15 shows the average visual benefit in the sample of four kerataconics for the three pupil sizes. These patients can expect a large benefit at all pupil sizes. Based on this information, the development of technologies to correct the idiosyncratic higher-order aberrations of such patients would be an especially valuable outcome of wavefront sensing. The wavefront sensor coupled with calculations such as these can efficiently screen those patients who stand to gain the largest benefit from customized correction.

The Visual Benefit of Higher-Order Correction Measured With Adaptive Optics

The analysis so far has been based on calculation and theory. It would be helpful if a reliable, noninvasive method existed that allowed higher-order aberrations to be quickly corrected in normal eyes, so that the actual visual benefit could be assessed. Fortunately, adaptive optics provide just such a method. Figure 3-16 shows a simplified drawing of an adaptive optics system for the eye that is in use in our lab at the University of Rochester.[12,45] The complete system requires a wavefront sensor to measure the wave aberration of the eye and a wavefront corrector to compensate for the aberrations.

The correcting element in our system is a deformable mirror with 97 actuators (or small mechanical pistons) mounted behind it that can reshape the mirror in such a way as to temporarily correct most of the particular aberrations found in each patient's eye.

In addition to the wavefront sensor and corrector, the adaptive optics system has an optical path that allows the subject to view visual stimuli, such as sine wave gratings or Snellen letters, through the deformable mirror.

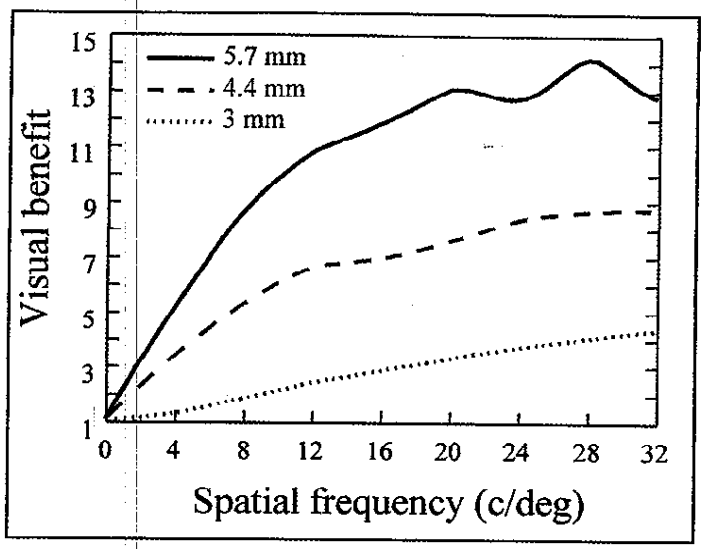

Figure 3-15. Average visual benefit in a sample of four kerataconic patients, for three pupil diameters.

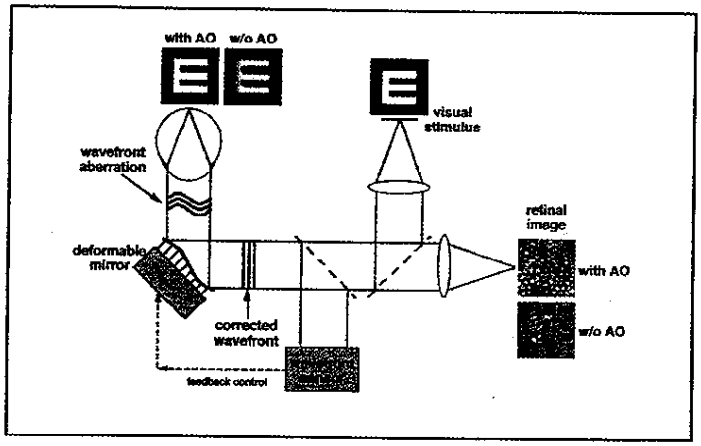

Figure 3-16. Schematic of the University of Rochester adaptive optics system for the human eye.

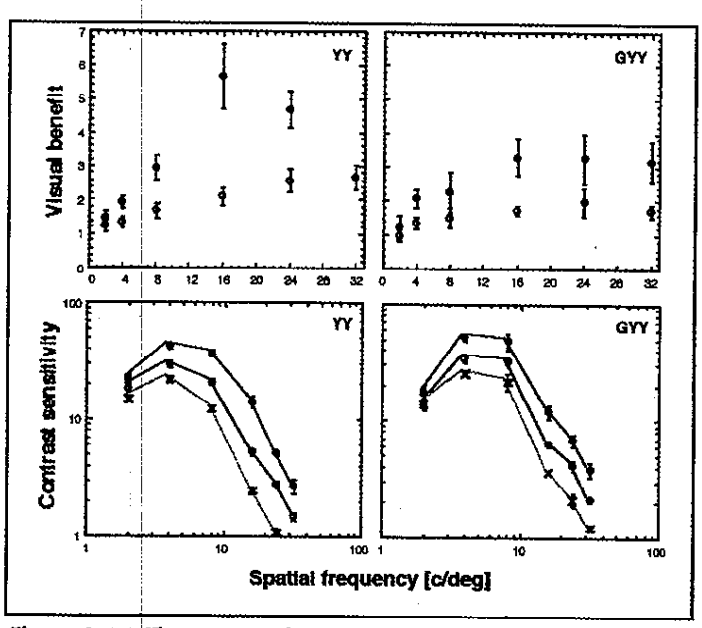

Figure 3-17. The measured contrast sensitivity (lower panels) and visual benefit (upper panels) for two subjects when correcting various aberrations across a 6 mm pupil: both monochromatic and chromatic aberrations (filled circles), monochromatic aberrations only (open circles), and defocus and astigmatism only (x symbols).

Subjects viewing the world through adaptive optics can have a sharper image of it than they have ever had before. Adaptive optics can also correct the aberrations for light leaving the eye, which makes it possible to obtain very high resolution images of the living retina[46] as well as to improve vision.

Contrast Sensitivity With and Without Higher-Order Correction

To assess the benefit of correcting higher-order aberrations, we measured the contrast sensitivity of the eye following correction with adaptive optics compared with the contrast sensitivity following a conventional refraction to correct defocus and astigmatism only. Figure 3-17 shows the CSF (lower panels) and visual benefit (upper panels) for two subjects with only defocus and astigmatism corrected (x symbols), after correcting the higher-order monochromatic aberrations as well as defocus and astigmatism (open circles), and after correcting both monochromatic aberrations and chromatic aberration (filled circles). In this case, visual benefit is calculated from the ratio of the CSFs instead of the ratio of MTFs, but its meaning is otherwise identical. Chromatic aberrations, both axial and transverse, were eliminated by placing a narrow band interference filter between the eye and the stimulus.

The results are similar for both subjects. The contrast sensitivity when correcting most monochromatic aberrations with a deformable mirror is higher than when defocus and astigmatism alone are corrected. This illustrates that higher-order aberrations in normal eyes reduce visual performance. Moreover, correcting both chromatic and monochromatic aberrations provides an even larger increase in contrast sensitivity.

Figure 3-17 also shows the visual benefit of correcting various aberrations, defined as the ratio of contrast sensitivity when correcting monochromatic and chromatic aberrations (filled circles) and when correcting monochromatic aberrations only (open circles) to that when correcting defocus and astigmatism only. Contrast sensitivity when correcting monochromatic aberrations only is improved by a factor of 2 on average at 16 and 24 c/deg. The maximum visual benefits for the two subjects are approximately a factor of 5 (YY) and 3.2 (GYY) at 16 c/deg when both monochromatic aberrations and chromatic aberration were corrected.

The Role of Chromatic Aberration

These results illustrate that the maximum increase in retinal image contrast that could be achieved requires correcting the chromatic aberrations as well as the monochromatic aberrations. Figure 3-18 shows the average maximum theoretical visual benefit computed from the wave aberrations of 17 subjects for a 6 mm pupil. Correcting monochromatic aberrations alone provides a large benefit of a factor of about 5 at middle and higher spatial frequencies.

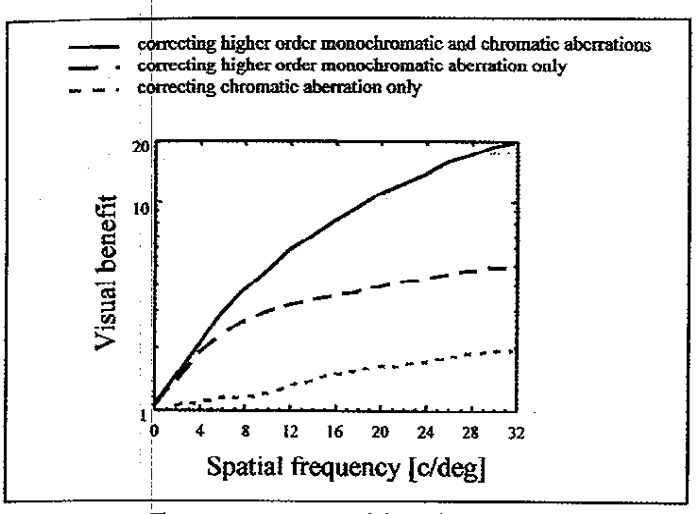

Figure 3-18. The maximum visual benefit of correcting higher-order monochromatic aberrations and/or chromatic aberration for a 6 mm pupil. A perfect correction method was assumed. The monochromatic MTFs were computed every 10 nm from 405 to 695 nm assuming an equally distributed energy spectrum. The reference wavelength assumed to generate no chromatic aberration was 555 nm where the photopic spectral sensitivity is maximal. The axial chromatic aberration data of Wald and Griffin[42] was used after rescaling it to the reference wavelength of 555 nm. Estimates of foveal transverse chromatic aberration from Thibos et al[47] were also considered in the calculation. For both monochromatic and white light conditions, the amounts of defocus were chosen to maximize the MTF at 16 c/deg.

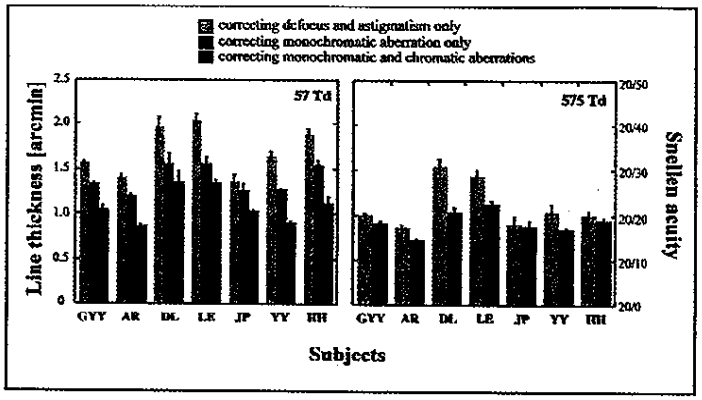

Figure 3-19. Measured visual acuity for seven subjects when correcting various aberrations for a 6 mm pupil. Two retinal illuminance levels, 57 (left) and 575 Td (right), were used. A color cathode ray tube (CRT) was used to display the acuity target, a single letter E. The spectrum of the CRT was a reasonable example of the broadband spectrum considered in natural scenes. The letter E with one of four different orientations was displayed at 100% contrast. From trial to trial, the orientation of the letter was varied randomly among four orientations: the normal orientation and rotations of 90, 180, and 270 degrees. Subjects indicated the orientation of the letter by pressing one of four keys. The psychometric function based on 40 trials was derived using the QUEST procedure[50] and acuity was taken as the line thickness of the letter for which 82% of responses were correct. Chromatic aberration was removed using a 10 nm bandwidth interference filter.

The theoretical benefit of correcting both chromatic and monochromatic aberrations is substantially larger than that when correcting higher-order monochromatic aberrations alone.

In theory for these subjects, correcting both could increase contrast sensitivity by a factor of almost 20 at 32 c/deg. These theoretical benefits are larger than we measured empirically (see Figure 3-17) because the adaptive optics system is incapable of perfect correction.

Campbell and Gubisch found that contrast sensitivity for monochromatic yellow light, which cannot produce chromatic aberration, was only slightly greater than contrast sensitivity for white light.[48] One of the reasons that axial chromatic aberration is not as deleterious under normal viewing conditions as one might expect is that it is overwhelmed by the numerous monochromatic aberrations.[49] This is shown in Figure 3-18. The visual benefit when only chromatic aberration is corrected is relatively small since the effect of higher-order aberrations on retinal image quality dilutes the benefit of correcting chromatic aberration. There is a larger gain when monochromatic aberrations are corrected without correcting chromatic aberration. Correcting both at the same time produces even larger benefits. The challenge is to devise a method to correct the chromatic aberrations of the eye along with the monochromatic aberrations. This cannot be achieved with laser refractive surgery. Multilayer contact lenses that could correct chromatic aberration with conventional methods would be too bulky, and decentration would obliterate any benefit. Reducing the bandwidth of illumination is simple to implement and is effective, but it also eliminates color vision and greatly reduces luminance. No practical solution to this problem currently exists. Even if it did exist, as we will see later, perfect correction of all aberrations does come at the expense of depth of field.

Snellen Acuity With and Without Higher-Order Correction

Due to the ubiquitous use of Snellen acuity in the clinic, we have also measured the increase in Snellen visual acuity provided by correcting higher-order aberrations as well as defocus and astigmatism. Figure 3-19 shows visual acuity at a low (mesopic, 57 Td, left) and a high (photopic, 575 Td, right) retinal illuminance. Before the measurement, defocus and astigmatism were subjectively corrected with a trial lens, if necessary. Correcting monochromatic aberrations provides an average increase for the seven subjects of a factor of 1.2 at 575 Td and 1.4 at 57 Td. All subjects reported an obvious subjective increase in image sharpness when higher-order aberrations were corrected compared with the conventional refraction. Correcting both monochromatic and chromatic aberrations improves visual acuity by a factor of 1.6. Therefore, visual acuity reveals a small benefit of correcting higher-order monochromatic aberrations.

Though the reliable improvements in letter acuity can be measured when higher-order aberrations are corrected with adaptive optics, visual acuity is a far less sensitive measure of the benefits of correcting higher-order aberrations than contrast sensitivity.

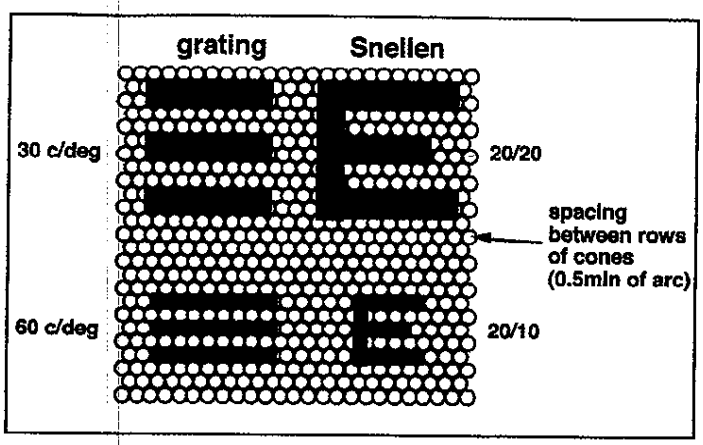

Figure 3-20. The grating and the Snellen letter E sampled by the foveal cone mosaic with a triangular arrangement. 20/20 vision (5 minutes of visual angle) and 20/10 vision (2.5 minutes) roughly correspond to 30 c/deg and 60 c/deg, respectively. The spacing between cones is about 0.5 minutes.

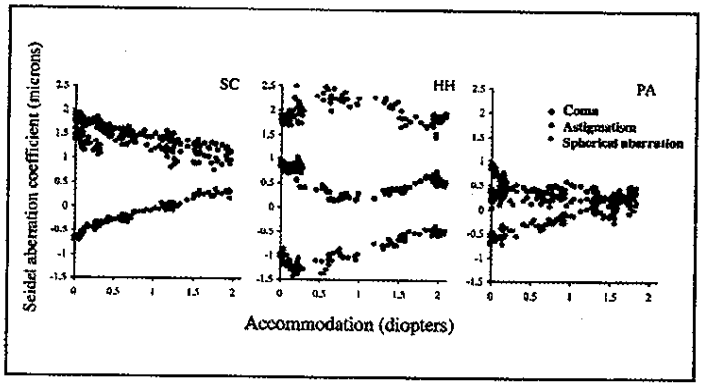

Figure 3-21. Changes in some of the eye's aberrations with accommodation. Pupil size is 4.7 mm. The Seidel aberrations were calculated from wave aberration measurements made with a real-time Shack-Hartmann wavefront sensor at a rate of 25 Hz while the subjects smoothly changed accommodation from the far point to a vergence of about 2 D.

This is because the contrast sensitivity curve is steep at the acuity limit and a large increase in contrast sensitivity slides the intersection of the curve with the x-axis only a short distance. Another reason why visual acuity may underestimate the benefit of correcting higher-order aberrations is that cone sampling considerations will ultimately limit acuity even when improvements in retinal image contrast can continue to provide improved contrast sensitivity at lower spatial frequencies. How does Snellen acuity compare with grating acuity? (see Chapter 7) Figure 3-20 shows a mosaic of foveal cones assuming a triangular arrangement, the 20/20 and the 20/10 letters E, and gratings of 30 and 60 cycles/deg. Approximately an array of 10 x 10 cones samples the 20/20 letter. Clinical visual acuity is usually defined as letter acuity using a standard letter chart observed at a set distance. The size of the smallest letter that can be recognized is taken as the clinical visual acuity of the subject. The most widely used system of acuity notation is the Snellen fraction: V = d/D, where d is distance at which a given letter can just be discriminated and D is distance at which the same letter subtends 5 minutes of arc of visual angle. The reading distance is usually 6 meters (m) (20 feet [ft]). At that distance, the letter size corresponding to 20/20 vision (6/6 in m) is 5 minutes of arc in height. Acuity of 20/200 means that the subject can read at 20 ft a letter that subtends 5 minutes at 200 ft (ie, the smallest letter that this subject can read at 6 m would subtend 50 minutes). A subject subtends 2.5 with 20/10 vision could read at 6 m a letter that subtends 2.5 minutes of arc. The 20/20 letter E may be regarded as being composed of three black horizontal lines and two interdigitated white lines, which have the same spacing as a grating with a spatial frequency of 0.5 c/min, or 30 c/deg. A 20/10 letter has the same stroke periodicity as a 60 c/deg grating. If human grating acuity approaches 60 c/deg, one may well wonder why the average Snellen acuity is not 20/10. For one thing, the detection of gratings is a very different task than the recognition of Snellen letters. In Snellen acuity, the subject can be influenced by literacy and past experience. Letters present low spatial frequency cues due to the symmetry or asymmetry in the form that can help recognize them. Grating targets usually extend over a larger visual angle than their equivalent Snellen letters, which increases their visibility. All these factors make the comparison between Snellen and grating acuity problematic. As mentioned above, increasing retinal image quality with higher-order correction generally is expected to have a smaller effect on high contrast visual acuity than contrast sensitivity, whether measured with gratings or letters. We suggest that visual benefit, as we have defined it based on retinal image contrast, is a more robust and useful measure of the outcome of correcting higher-order aberrations. If an acuity measure is to be used, an alternative is low contrast visual acuity, which should be more sensitive than high contrast visual acuity.

Additional Considerations in Higher-Order Correction

We have already discussed the role that pupil diameter and chromatic aberration play in the visual benefit of higher-order correction. This section discusses additional factors that need to be considered to evaluate the ultimate benefits that customized correction will be able to produce.

Accommodation

Any attempt to improve the eye's optics with a customized correction will only be beneficial if the values of the eye's aberrations are relatively fixed. If, for any reason, the eye's optics are not stable, the ability to improve vision will be limited. The eye's higher-order aberrations change substantially with accommodation. What implications will this have for the visual benefit that could be obtained with a customized correction? Figure 3-21 shows how a few of the eye's aberrations—coma, astigmatism, and spherical aberration—varied for a 4.7 mm pupil in three subjects as they smoothly changed their accommodation from distant (far point) to near accommodation (a change of about 2 D or 0.5 m).[51] Although the nature of the change in the eye's higher-order aberrations generally varies for different subjects, it is clear that for each subject there are substantial, systematic changes in the aberrations that depend on accommodative state. This means that a higher-order correction tailored for distance vision would not be appropriate for near viewing and vice versa.

For the same three subjects, the effect of accommodative state on the monochromatic visual benefit that could be attained with a higher-order correction is illustrated in Figure 3-22. The blue

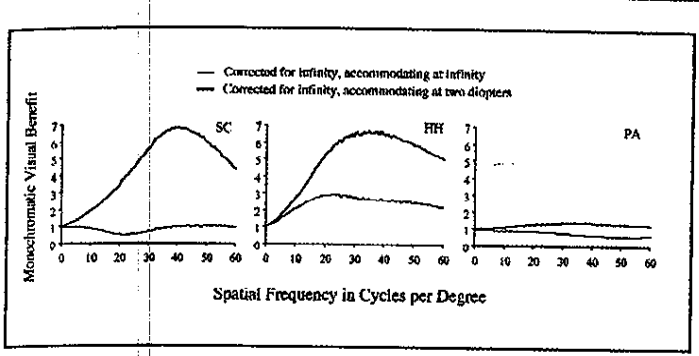

Figure 3-22. The effect of accommodative state on visual benefit. For the same three subjects as in Figure 3-21, the visual benefit in monochromatic light was computed for different accommodative states from wave aberrations measured with a Shack-Hartmann wavefront sensor. Pupil size is 4.7 mm.

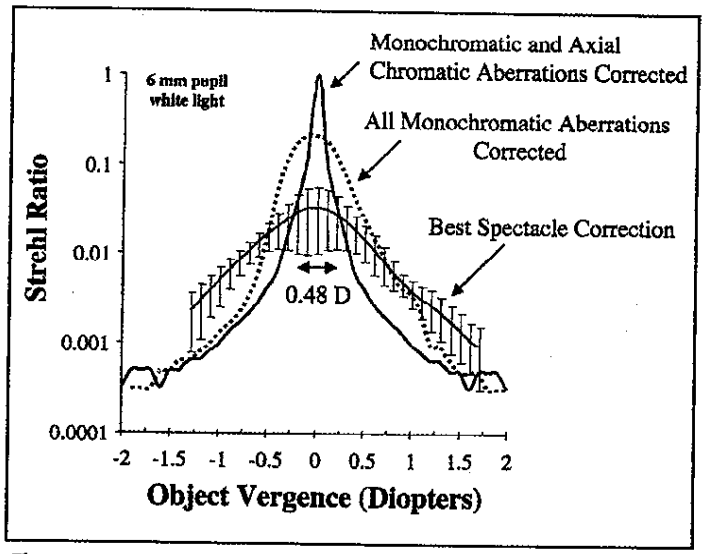

Figure 3-23. Average changes in the Strehl ratio as a function of light vergence in white light when correcting defocus and astigmatism alone (solid red curve), when correcting all monochromatic aberrations (dotted blue curve), and when correcting both monochromatic and axial chromatic aberrations (solid black curve). These data were calculated based on wave aberration measurements obtained from 13 eyes and incorporated axial chromatic aberration (6 mm pupil). Correcting higher-order aberrations increases image quality over a 1.25 D range, but results in worse image quality outside of this range when compared with a spectacle correction. Correcting both monochromatic and chromatic aberrations can optimize image quality at the expense of a further reduction in the depth of focus.

curve for each subject shows the visual benefit that would be obtained with the ideal corneal ablation profile designed to eliminate the eye's higher-order aberrations when the subject is accommodating at infinity. This is the maximum obtainable visual benefit for each subject. The pink curve shows the subject's visual benefit obtained with this same ablation profile, but now when the subject is actually accommodating at 2 D instead of infinity. It is important to keep in mind that defocus is not responsible for the drop in visual benefit. In fact, it has been assumed that the subject has perfect accommodation. This was implemented by zeroing the residual Zernike defocus. (*Note*: although the focal plane for best image quality does not necessarily correspond to the plane where Zernike defocus is equal to 0, for relatively small pupil sizes and mild wave aberrations, zeroing the Zernike defocus is usually a good approximation to the best focal plane.) This shows that a customized corneal ablation profile tailored to perfectly correct all higher-order aberrations at one accommodative state will be less effective when the accommodative state is substantially changed. In this situation, the custom correction is little better, and maybe even somewhat worse, than a traditional spherocylindrical correction. Though the changes of the wave aberration with accommodation limit the conditions under which a customized static correction of the eye's aberrations would provide a benefit in young people who can still accommodate, it does not imply that such a correction would have no use. This limitation is not particularly severe because it does not apply to presbyopes. Even in younger people, there would be value in designing a lens to correct for distance vision.

The failure to focus correctly on the target, or accommodative lag, will also diminish the visual benefit of higher-order correction. Accommodative lag typically increases as the luminance of the stimulus is reduced and can yield an error in defocus of 0.3 D or more in low luminance conditions.[52] We showed in Figure 3-10 that the image blur produced by 0.3 D of defocus is nearly identical to that produced by the higher-order aberrations alone. This implies that one needs to maintain accurate accommodation in order to reap the full benefit of a customized higher-order correction. An error as slight as 0.3 D in a patient's ability to focus in dim lighting conditions will greatly reduce the visual benefit obtained by correcting the eye's higher-order aberrations, which are highest for large pupil diameters. Despite these limitations, we believe that it is advantageous to correct for higher-order aberrations generally for distance corrections because the pupil constricts with accommodation, making higher-order aberrations less problematic.

Depth of Focus

A customized correction of higher-order aberrations may also reduce the eye's depth of focus. We can see this effect in Figure 3-23, which illustrates how the eye's Strehl ratio changes as a function of light vergence for three separate conditions in white light (6 mm pupil). The Strehl ratio is an image quality metric defined as the ratio of the peak value of the eye's PSF with aberrations to that of a diffraction-limited system. A perfect, diffraction-limited system has a Strehl ratio of 1, with image quality typically becoming worse as the Strehl ratio approaches 0. As shown in Figure 3-23, correcting all of the eye's monochromatic aberrations improves image quality over a range of nearly 1.25 D, outside of which image quality is actually better with a conventional spectacle correction. Correcting all of the eye's monochromatic and axial chromatic aberrations can yield the highest Strehl ratio and best image quality at the expense of an additional reduction in the depth of focus (0.48 D range). An analysis of the real impact of a reduction in the eye's depth of field with higher-order correction has yet to be performed.

Slow Changes in the Wave Aberration Over Time

Another issue that is important to consider in evaluating the feasibility of a customized corneal ablation procedure is whether, for a fixed accommodative state, the wave aberration is stable over long periods of time. If higher-order aberrations were not

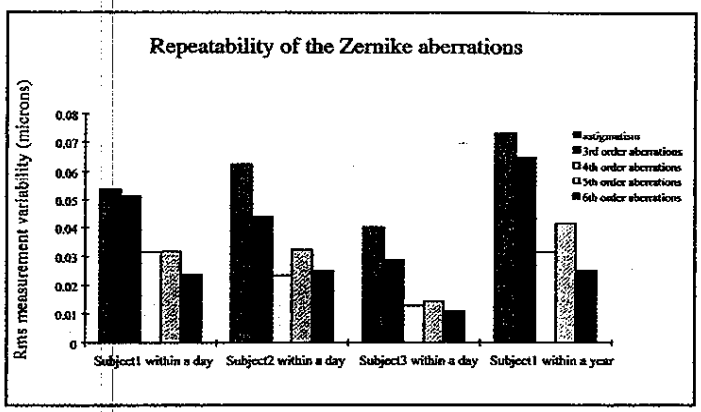

Figure 3-24. Repeatability of the Zernike aberration measurement for Zernike coefficients of different radial orders. This figure shows the average RMS variability of different orders of Zernike coefficients measured several times throughout a single day for three subjects. Pupil size was approximately 6 mm. The RMS measurement variability of the different Zernike orders over the course of 1 year is also shown for one of the subjects. The Zernike coefficients were measured with a Shack-Hartmann wavefront sensor. Since the measurement variability includes experimental errors specific to the particular Shack-Hartmann wavefront sensor, measurement noise, and errors due to pupil centration, it represents an upper boundary to the actual instability in the wave aberration.

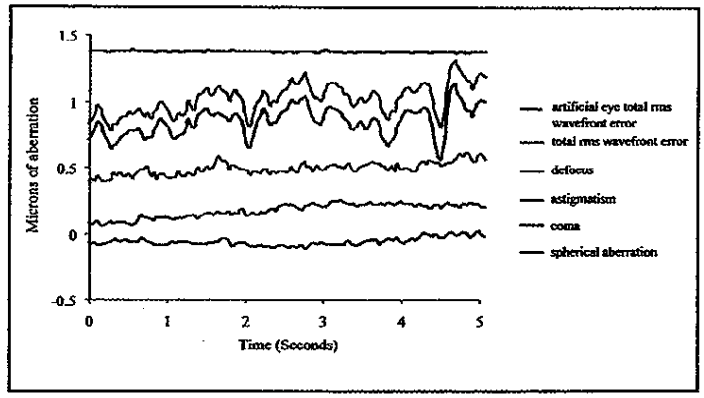

Figure 3-25. Short-term temporal instability in the eye's wave aberration. Aberrations were measured with a real-time Shack-Hartmann wavefront sensor while the subject attempted to fixate steadily on a high contrast target at 2 D. Pupil size is 4.7 mm.

stable, there would be little point in performing a customized corneal ablation. This issue can be addressed by examining the repeatability with which the wave aberration can be measured within a single day and within an entire year. Figure 3-24 shows the RMS between-measurement variability in the wave aberration, expressed in microns, for three subjects with 6 mm pupils. Each measurement was made with a long integration time to minimize the influence of short-term instability in the wave aberration, to be discussed later. Within-a-day variability depends on the Zernike order considered, but generally ranges between 0.01 and 0.06 μm. This RMS within-a-day variability is about nine times smaller than the average magnitude of aberration for the second-order aberrations and about three times smaller than the average magnitude of aberration for the third- and fourth-order modes. It is likely that the actual variability in the wave aberration is smaller than this since much of the variability is probably due to changes in pupil position and other sources of measurement error rather than actual changes in the wave aberration that would affect vision.

Figure 3-24 also shows repeatability data for one eye over a much longer time scale. The wave aberration for this eye was measured on three occasions spanning more than an 8-month period, and showed a RMS between-measurement variability of less than 0.08 μm in every case, only slightly worse than the within-a-day variability, both of which are minimal. These results imply that, for a fixed accommodative state, the wave aberration of the eye is stable both within a day and probably over a period of many months as well. Although similar data for more subjects would be required to make a definitive statement about longer periods, the evidence that is available indicates that a custom surgical procedure to correct higher-order aberrations would be of value to the patient for an extended period of time.

The evidence that is available indicates that a custom surgical procedure to correct higher-order aberrations would be of value to the patient for an extended period of time.

Although we believe the wave aberration to be fairly stable over relatively long time periods, it is known that spatial vision does deteriorate with age.[53] In addition to neural factors, a significant steady increment in ocular aberrations with age has been found,[54,55] which produces a degraded retinal image in the older eye. Both changes in the crystalline lens[56,57] and changes in the cornea[58,59] are responsible. However, the cause of the degradation of the eye's optical quality is the loss of the aberration balance between cornea and lens that seems to be present in the younger eye.[60] These factors may ultimately limit the longevity of an effective customized correction and suggest that an adjustable customized correction would be optimal.

Rapid Changes in the Wave Aberration Over Time

The experiments described above address the issue of the long-term stability of the wave aberration, but they do not consider the possibility that the short-term stability of the eye might be poor. Rapid temporal fluctuations in the wave aberration might also reduce the value of a static correcting procedure such as a customized corneal ablation. All the calculations described thus far have assumed that the eye's aberrations are perfectly static in time, and the contrast sensitivity measurements described earlier are usually conducted with paralyzed accommodation so that at least some of the dynamics would have been suppressed compared with normal viewing.

Microfluctuations in accommodation, even during attempted steady-state accommodation, have been documented and studied since 1951;[61,62] however, measurement of the short-term instability of the eye's higher-order aberrations has not been possible until recently. Figure 3-25 shows the short-term temporal variability of the eye's total RMS wavefront error and of some of the Zernike aberrations for one subject measured over 5 seconds. For comparison, the total RMS wavefront error measured for a static artificial eye is also shown.[63] It can be seen from this figure that the eye's higher-order aberrations do exhibit temporal instability.

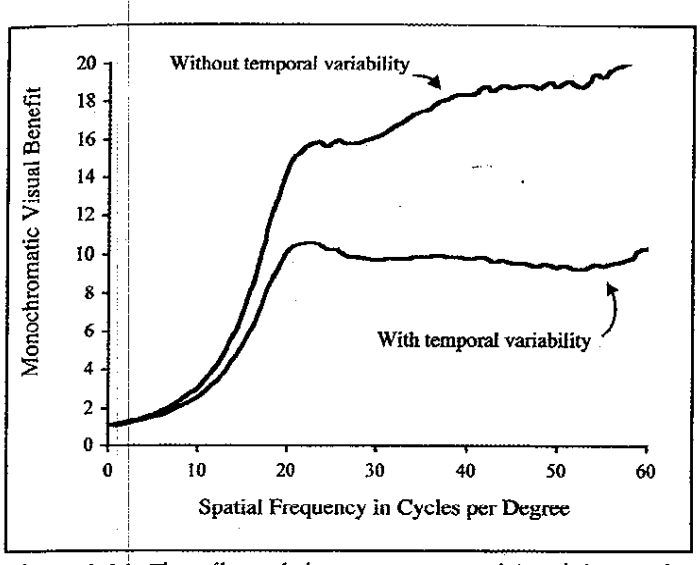

Figure 3-26. The effect of short-term temporal instability in the eye's wave aberration on the visual benefit of a perfect custom correction. The time-averaged monochromatic visual benefit for different conditions was calculated from wave aberration measurements made with a real-time Shack-Hartmann wavefront sensor. Pupil size is 5.8 mm. The blue curve is the benefit that could be obtained in the absence of temporal instability; this is the benefit that would be achieved with a perfect customized correction. The pink curve is the visual benefit obtained with a perfect customized correction of the static component of the eye's wave aberration when the effects of temporal instability are included; it is the best optical quality that can be achieved with any static correction method.

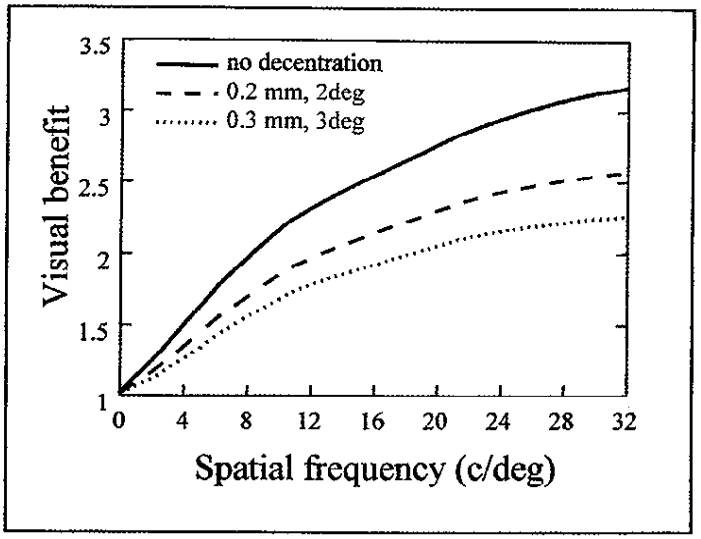

Figure 3-27. Mean visual benefit in white light across 10 eyes with 7 mm pupils, calculated when an ideal correcting method is perfectly centered and for decentrations within an interval of translation and rotation characterized with a standard deviation of 0.2 mm, 2 deg, and 0.3 mm, 3 deg, respectively. The visual benefit was obtained as the ratio between the MTF in white light when the monochromatic aberrations are corrected and the MTF achieved with an optimum correction of defocus and astigmatism.

By far the largest source of short-term instability in the eye's wave aberration is due to the microfluctuations in accommodation (or defocus).

Figure 3-26 shows the theoretical effect of this short-term variability in the eye's aberrations on the maximum visual benefit that can be obtained in one subject with a perfect customized corneal ablation procedure for a 5.8 mm pupil. The calculations were performed assuming a perfect correction of the static component of the eye's wave aberration and also perfect correction of the eye's chromatic aberration, implying that a perfect corneal ablation procedure, in the absence of temporal instability, would result in diffraction-limited performance. The effect of temporal instability is similar to the effect of chromatic aberration in that it only fully reveals itself when higher-order aberrations are very small. The blue curve indicates the monochromatic visual benefit of a perfect correction, for this subject, if the aberrations were perfectly static. The pink curve shows how the visual benefit is decreased when the effect of the temporal instability in the wave aberration is taken into account. Temporal instability causes very little reduction in visual benefit for the low spatial frequencies and a reduction of about a factor of 2 at higher spatial frequencies. Even so, the visual benefit for the perfect custom correction of the eye's static aberrations (pink curve) is still quite substantial, indicating that a perfect customized correction would still be of benefit to this subject.

Decentration Errors

The benefit from the correction of the higher-order aberrations will be reduced by decentrations of the correcting method. A customized contact lens will translate and rotate to some extent with respect to the cornea. Also, the eye is not completely static during a laser refractive surgery procedure. Calculations for an ideal correcting phase-plate model suggest, contrary to what one might expect, that reasonable decentrations do not detract greatly from the potential benefit of correcting higher-order aberrations.[64,65] Even with fixed translations or rotations of up to 0.6 mm and 30 degrees, a correction of the higher-order aberrations would still yield an improvement over a typical spherocylindrical refraction.

Even with fixed translations or rotations of up to 0.6 mm and 30 degrees, a correction of the higher-order aberrations would still yield an improvement over a typical spherocylindrical refraction.

Maximum translations and rotations reported for soft contact lenses[66] and measurements of the motion of the eye during the laser surgery treatment[67] allow us to estimate the typical decentration of an ideal correcting method. Figure 3-27 shows the impact of movements within a reasonable interval (characterized by a standard deviation of 0.2 to 0.3 mm for translation, and 2 to 3 degrees for rotation) on the visual benefit in white light. The eye's chromatic aberration overwhelms the effect of residual aberrations caused by decentrations. The visual benefit is as high as 2.50 at 32 c/deg, only somewhat less than the ideal case with no decentration.

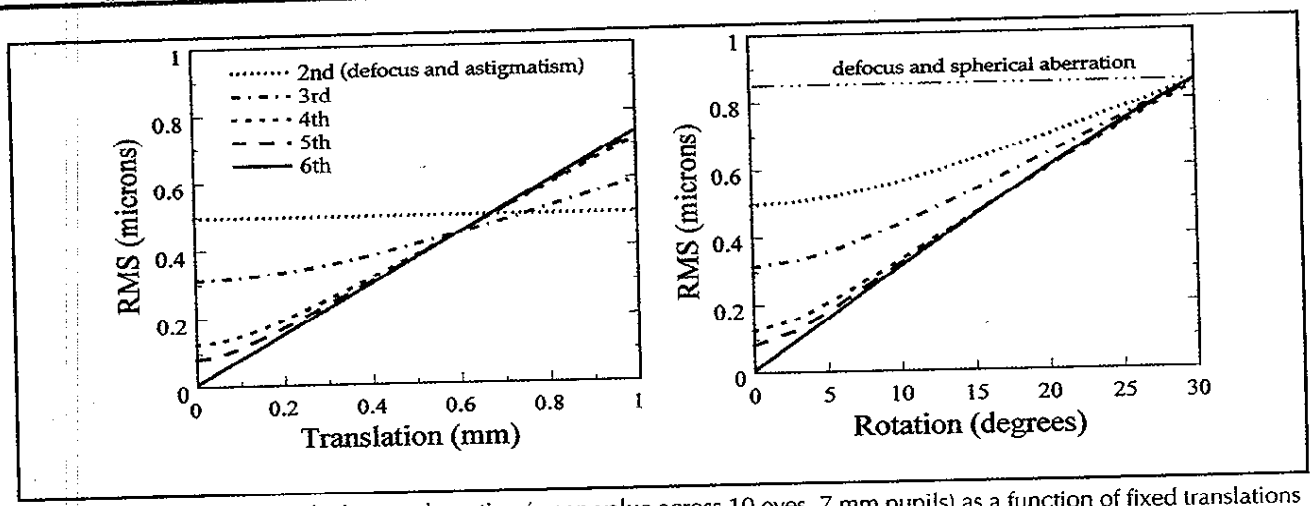

Figure 3-28. RMS of the residual wave aberration (mean value across 10 eyes, 7 mm pupils) as a function of fixed translations and rotations, when the ideal correcting method corrects the higher-order aberrations up to second, third, fourth, fifth, and sixth order. For example, a method designed to compensate for the aberrations up to fourth order leaves uncorrected the aberrations higher than fourth order and there is a residual RMS even with perfect centration due to the incomplete correction. The RMS is a measure of the total amount of aberration.

Correcting progressively higher orders of aberration will result in progressively lower tolerances to decentration. Figure 3-28 shows the impact of translation and rotation on a correction that includes different orders of aberration (up to second, third, fourth, fifth, and sixth order). The ordinate is a measure of the amount of residual aberrations remaining in the eye. While a perfectly centered correcting method continues to provide improvement in image quality when it is designed to correct more orders, the benefit of correcting additional orders decreases when decentration increases. This fact indicates that the higher-order corrections are more sensitive to translation and rotation. If the expected decentration of the correction is too large, then it is not worth correcting all the higher-order aberrations that one can measure.

So, in general as a general statement, nearly 50% of the eye's higher-order aberrations would still be eliminated in a customized correction that was statically translated by 0.25 to 0.5 mm and rotated by 8 to 10 degrees.

Of course, the types of decentrations that typically occur during laser in-situ keratomileusis (LASIK) are not necessarily as simplistic as the previously considered model in which the entire higher-order correction has been statically displaced and/or rotated on the eye. Dynamic eye movements in a conventional or customized procedure can also introduce additional aberrations in laser refractive surgery. Finally, another important caveat is that the process of removing corneal tissue in refractive surgery could also induce other aberrations not accounted for in the phase-plate model.

Effect of Beam Size on Customized Refractive Surgery

The success of customized laser refractive surgery depends on using a laser beam that is small enough in diameter to produce the fine ablation profiles needed to correct the eye's higher-order aberrations. Just as an artist requires a finer paintbrush for more detailed work, the laser refractive surgeon requires a smaller diameter laser beam to achieve a successful customized ablation. Based on wave aberration data from real eyes, we theoretically calculated the effect of changing the laser beam size on the expected benefit of a customized refractive surgery procedure.[68] We calculated the residual aberrations that would remain in the eye for beam diameters ranging from 0.5 to 2 mm, estimated retinal image quality, and conducted a Fourier analysis to study the spatial filtering properties of each beam size. The laser beam acts like a spatial filter, smoothing the finest features in the ablation profile. The quality of the customized correction declines steadily when the beam size increases, as large diameter laser beams decrease the ability to correct finer, higher-order aberrations in the eye.

A beam diameter of 2 mm is capable of correcting defocus and astigmatism while beam diameters of 1 mm or less may effectively correct aberrations up to fifth order. A top-hat laser beam of 1 mm (or an equivalent Gaussian profile with a full-width at half maximum [FWHM] of 0.76 mm) is small enough to achieve a customized ablation for typical human eyes.

For more information on the requirements for a customized correction of the eye's aberrations, refer to Chapter 22.

The Rationale for Pursuing Higher-Order Correction

Even though we must consider the implications of the aforementioned hurdles in the path to effective customized correction, it is clear from the population statistics that substantial benefits can be had for some eyes in the normal population. As previously shown in Figure 3-13, there are some subjects who have a visual benefit of nearly 1, indicating that they have excellent optics and would not benefit from a customized correction. However, there are also many normal subjects who possess inferior optical quality and would experience large visual benefits from a customized correction, particularly for large pupil sizes (such as in nighttime con-

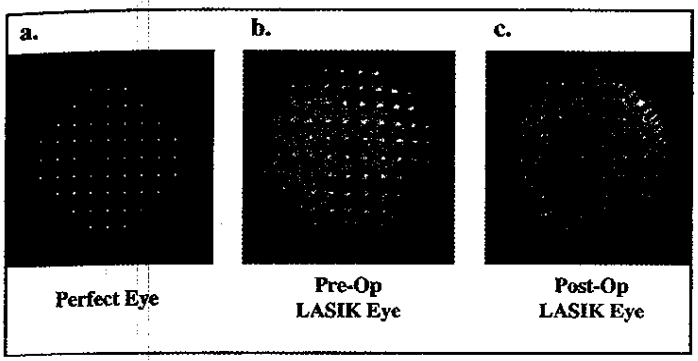

Figure 3-29. The Shack-Hartmann spot array pattern for a perfect eye (A), a normal aberrated eye (B), and the same eye following LASIK surgery (C).

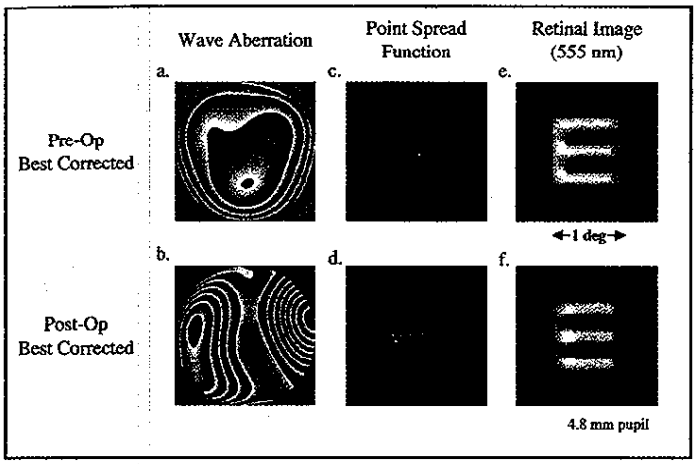

Figure 3-31. The wave aberrations across a 4.8 mm pupil for the same LASIK patient's left eye before surgery with his best correction (A) and after surgery with his best correction (B), and his corresponding PSFs (C and D). The aberrations have become more severe for the patient over this moderately larger pupil diameter. For the wave aberrations shown in (A) and (B), the subject's best refraction was again determined by adjusting the amount of defocus and astigmatism needed to maximize the Strehl ratio in their corresponding PSF. The patient's best corrected PSF before and after surgery was convolved with the letter E in monochromatic light (555 nm) to produce the retinal image shown in (E) and (F). After surgery, higher-order aberrations become the dominant source of degradation in the quality of the letter E.

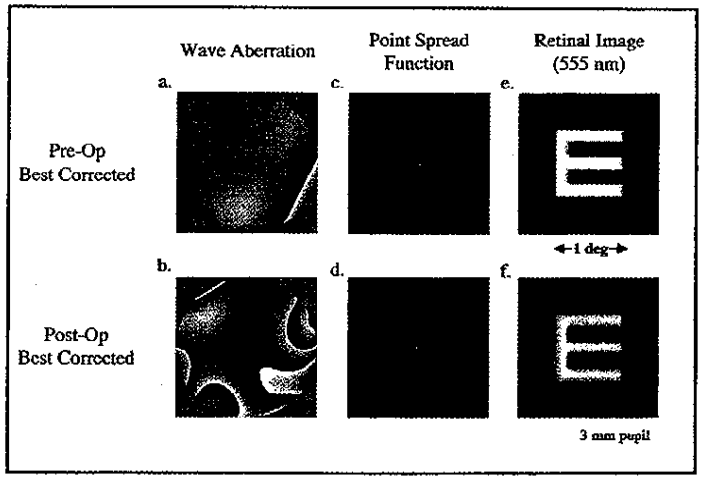

Figure 3-30. The wave aberrations across a 3 mm pupil for the LASIK patient's left eye before surgery with his best correction (A) and after surgery with his best correction (B), and his corresponding PSFs (C and D). For the wave aberrations shown in (A) and (B), the subject's best refraction was determined by adjusting the amount of defocus and astigmatism (or all three second-order Zernike modes) needed to maximize the Strehl ratio in their corresponding PSF. (E) and (F) show the result of convolving the letter E in monochromatic light (555 nm) with the patient's best corrected PSF before and after surgery. After surgery, higher-order aberrations become the dominant source of degradation in the quality of the letter E.

ditions). Of course, pathological patients, such as keratoconics, would experience the greatest gains in visual performance.

In addition to correcting higher-order aberrations in these populations, it is important to examine and attempt to correct for the higher-order aberrations that are being introduced by current refractive surgical procedures. Figure 3-29 shows three images obtained from a Shack-Hartmann wavefront sensor. The details of its operation will be explained in Chapter 7. A perfect eye, shown in Figure 3-29A, produces a spot pattern that is regular and possesses uniform spots that are equally spaced. An aberrated eye produces a Shack-Hartmann array containing spots that are displaced from their ideal, perfect locations. The larger the displacements of these spots, the greater the amount of aberration that is present in an image. Adjacent to the perfect eye is the Shack-Hartmann array for the patient before LASIK surgery. The preoperative spherocylindrical refraction of this unoperated eye was -7.75 -2.00 x 57. The third picture in this sequence shows the Shack-Hartmann array for the same subject 4 months following LASIK surgery. The postoperative refraction for this LASIK eye was +0.25 -0.50 x 172. As seen in the figure, the spots in the center of the pupil are fairly uniform and evenly spaced while the spots in the periphery become distorted and elongated as the spacing between the spots becomes dramatically compressed. This indicates that the aberrations are becoming more severe as we move away from the center of the pupil, which is characteristic of the pin cushion appearance of spherical aberration.

We can more easily determine how the aberration structure of the patient has changed following surgery by analyzing the pre- and postoperative Shack-Hartmann arrays to determine the corresponding wave aberrations. These results are shown in Figure 3-30 for a 3 mm pupil diameter and in Figure 3-31 for a 4.8 mm pupil diameter. The step size of an individual contour line in the wave aberration is 0.56 μm. Due to the large compression and overlapping of the spots in the periphery of the postoperative eye, we were unable to accurately determine the wave aberration for pupil diameters larger than 5 mm. The eye's PSF for any pupil size up to 5 mm may then be determined from the wave aberration, yielding a complete description of the imaging properties of the entire eye.

For the smaller pupil size of 3 mm, we see that there is not a dramatic difference between the wave aberration before and after surgery. This is to be expected since the eye's aberrations are mainly limited by diffraction for small pupil diameters. By convolving the letter E with the eye's PSF, we can directly observe how the eye's wave aberration degrades the retinal image. Even for this small pupil size, the letter E shows a reduction in image quality

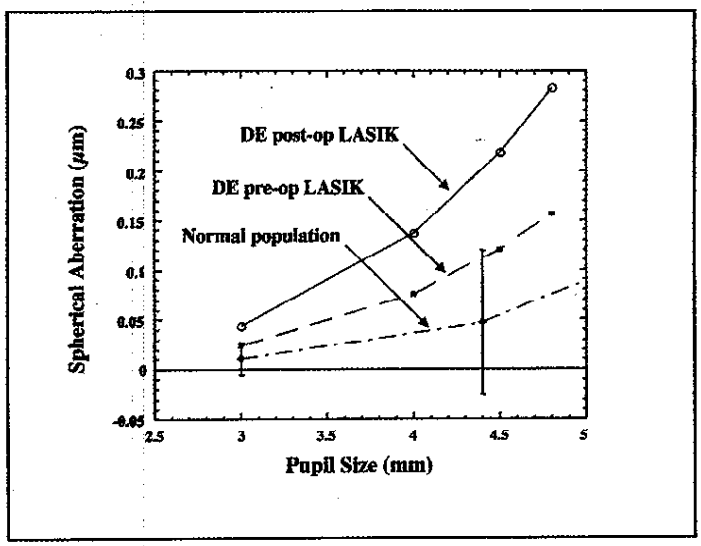

Figure 3-32. Spherical aberration (in microns) for the normal population of 109 subjects (dash-dotted blue line), the patient before LASIK surgery (dashed green line), and the patient after LASIK surgery (solid red line) as a function of pupil size. The error bars for the normal population represent plus and minus 2 standard deviations from the mean value, encompassing approximately 95% of the normal population. The patient's preoperative values for spherical aberration fit in with the normal population. However, after LASIK surgery, the patient's spherical aberration doubles in magnitude as a result of the procedure.

after surgery when compared with the preoperative E, indicating that the surgery has produced higher-order aberrations.

The same trends occur to a larger degree in Figure 3-31 for the 4.8 mm pupil. The best-corrected postoperative LASIK eye produces a retinal image of the letter E whose quality is inferior to that formed by the best-corrected preoperative eye. As the pupil size increases from 3 to 4.8 mm, the postoperative LASIK patient has noticeably poorer retinal image quality than his or her typical, unoperated eye and would see even worse for larger pupil diameters. The wave aberration after surgery for the postoperative LASIK eye is fairly smooth in the center of the pupil, as evidenced by the low density of contour lines. However, the density of the contour lines increases at the edge of the pupil, indicating the presence of more severe aberrations in the periphery of the pupil. This increase in aberration structure at the pupil edge is primarily due to a steepening of the cornea near the transition zone of the ablation.[69]

The predominant higher-order aberration exhibited by this LASIK patient and several other LASIK patients[69-71] after surgery is spherical aberration, which often increased two- to fourfold with conventional LASIK.

See Chapter 7 for similar evidence obtained from corneal topographic measurements. Corneal topography correlates with wavefront variance.[72]

Figure 3-32 shows the increase in spherical aberration for this LASIK patient as a function of pupil diameter. Before surgery, the preoperative values of spherical aberration for the patient are comparable to those expected from the normal population data. After surgery, the magnitude of spherical aberration in the post-LASIK eye becomes twice as large as the unoperated values. This postoperative value will become even larger as the pupil diameter increases from a moderate size of 4.8 mm to a fully dilated size of 6 or 7 mm, severely degrading nighttime vision.

The results from this LASIK patient and the population data suggest that there is a need to refine corrective techniques that can eliminate the eye's higher-order aberrations. Abnormal eyes, such as keratoconics, and eyes containing large amounts of higher-order aberrations, such as the patient discussed here, will obviously benefit the most from a customized correction. Normal eyes, particularly in low illumination conditions with large pupil diameters, can also substantially benefit from a customized correction. Wavefront sensing is a key technology that will be instrumental in optimizing these techniques to maximize the potential benefit each individual patient will be able to receive from a customized correction.

References

1. Willoughby Cashell GT. A short history of spectacles. *Proc Roy Soc Med.* 1971;64:1063-1064.
2. Rubin ML. Spectacles: past, present and future. *Surv Ophthalmol.* 1986;30:321-327.
3. Helmholtz H. *Helmholtz's Treatise on Physiological Optics.* New York: Optical Society of America; 1924.
4. Smirnov MS. Measurement of the wave aberration of the human eye. *Biophysics.* 1961;687-703.
5. Liang J, Grimm B, Goelz S, Bille J. Objective measurement of the wave aberrations of the human eye using a Shack-Hartmann wavefront sensor. *J Opt Soc Am A.* 1994;11:1949-1957.
6. Liang J, Williams DR, Miller DT. Supernormal vision and high-resolution retinal imaging through adaptive optics. *J Opt Soc Am A.* 1997;14:2884-2892.
7. Guirao A, Redondo M, Geraghty E, Piers P, Norrby S, Artal P. Corneal optical aberrations and retinal image quality in patients in whom monofocal intraocular lenses were implanted. *Arch Ophthalmol.* 2002;120(9):1143-1151.
8. MacRae SM, Schwiegerling J, Snyder R. Customized corneal ablation and super vision. *J Refract Surg.* 2000;16:S230-S235.
9. Mrochen M, Kaemmerer M, Seiler T. Wavefront-guided laser in situ keratomileusis: early results in three eyes. *J Refract Surg.* 2000;16:116-121.
10. Mrochen M, Kaemmerer M, Seiler T. Clinical results of wavefront-guided laser in situ keratomileusis 3 months after surgery. *J Cataract Refract Surg.* 2001;27:201-207.
11. Panagopoulou SI, Pallikaris IG. Wavefront customized ablations with the WASCA Asclepion workstation. *J Refract Surg.* 2001;17:S608-S612.
12. Liang J, Williams DR. Aberrations and retinal image quality of the normal human eye. *J Opt Soc Am A.* 1997;14:2873-2883.
13. Goodman JW. *Introduction to Fourier Optics.* 2nd ed. New York: McGraw-Hill; 1996
14. Williams DR. Topography of the foveal cone mosaic in the living human eye. *Vision Res.* 1988;28:433-454.
15. Williams DR, Coletta NJ. Cone spacing and the visual resolution limit. *J Opt Soc Am.* 1987;14:1514-1523.
16. Williams DR. Aliasing in human foveal vision. *Vision Res.* 1985;25:195-205.
17. Bergmann C. Anatomical and physiological findings on the retina. *Zeitschrift für rationelle Medicin II.* 1857;83-108.
18. Byram GM. The physical and photochemical basis of visual resolving power. Part II. Visual acuity and the photochemistry of the retina. *J Opt Soc Am.* 1944;34:718-738.
19. Campbell FW, Green DG. Optical and retinal factors affecting visual resolution. *J Physiol.* 1965;181:576-593.
20. Williams DR, Sekiguchi N, Haake W, Brainard D, Packer O. The cost of trichromaticity for spatial vision. In: Valberg A, Lee BB, eds. *From Pigments to Perception: Advances in Understanding Visual Processes.* Series A/Vol 203. New York: Plenum Press; 1991:11-22.

21. Østerberg GA. Topography of the layer of rods and ones in the human retina. *Acta Ophthalmol.* 1935;13:1-97.
22. Miller WH. Ocular optical filtering. In: Autrum H, ed. *Handbook of Sensory Physiology.* Vol VII/6A. Berlin: Springer-Verlag; 1979:70-143.
23. Yuodelis C, Hendrikson A. A qualitative analysis of the human fovea during development. *Vision Res.* 1986;26:847-856.
24. Curcio CA, Sloan KR, Packer O, Hendrickson AE, Kalina RR. Distribution of cones in human and monkey retina: individual variability and radial asymmetry. *Science.* 1987;236:579-582.
25. Curcio CA, Sloan KR, Kalina RR, Hendrickson AE. Human photoreceptor topography. *J Comp Neurol.* 1990;292:497-523.
26. Williams DR. Visibility of interference fringes near the resolution limit. *J Opt Soc Am A.* 1985;2:1087-1093.
27. Helmholtz H. *Popular Scientific Lectures.* New York: Dover Publications, Inc; 1962.
28. Van den Brink G. Measurements of the geometrical aberrations of the eye. *Vision Res.* 1962;2:233-244.
29. Berny F, Slansky S. Wavefront determination resulting from Foucault test as applied to the human eye and visual instruments. In: Dickenson JH, ed. *Optical Instruments and Techniques.* Newcastle, Del: Oriel Press; 1969:375-386.
30. Howland HC, Howland B. A subjective method for the measurement of monochromatic aberrations of the eye. *J Opt Soc Am.* 1977;67:1508-1518.
31. Walsh G, Charman WN, Howland HC. Objective technique for the determination of monochromatic aberrations of the human eye. *J Opt Soc Am A.* 1984;1:987-992.
32. Campbell MCW, Harrison EM, Simonet P. Psychophysical measurement of the blur on the retina due to optical aberrations of the eye. *Vision Res.* 1990;30:1587-1602.
33. Webb RH, Penney CM, Thompson KP. Measurement of ocular wavefront distortion with a spatially resolved refractometer. *Appl Opt.* 1992;31:3678-3686.
34. Platt B, Shack RV. Lenticular Hartmann screen. *Opt Sci Center Newsl.* 1971;5:15-16.
35. Howland HC, Buettner J. Computing high order wave aberration coefficients from variations of best focus for small artificial pupils. *Vision Res.* 1989;29:979-983.
36. Porter J, Guirao A, Cox IG, Williams DR. Monochromatic aberrations of the human eye in a large population. *J Opt Soc Am A.* 2001;18:1793-1803.
37. Thibos LN, Hong X, Bradley A, Cheng X. Statistical variation of aberration structure and image quality in a normal population of healthy eyes. *J Opt Soc Am A.* 2002;2329-2348.
38. Guirao A, Williams DR. A method to predict refractive errors from wavefront aberration data. *Optom Vis Sci.* In press.
39. El Hage SG, Berny F. Contribution of crystalline lens to the spherical aberration of the eye. *J Opt Soc Am.* 1973;63:205-211.
40. Artal P, Guirao A. Contribution of cornea and lens to the aberrations of the human eye. *Optics Letters.* 1998;23:1713-1715.
41. Artal P, Guirao A, Berrio E, Williams DR. Compensation of corneal aberrations by the internal optics in the human eye. *J Vision.* 2001;1:1-8.
42. Wald G, Griffin DR. The change in refractive power of the human eye in dim and bright light. *J Opt Soc Am A.* 1947;321-336.
43. Guirao A, Porter J, Williams DR, Cox IG. Calculated impact of higher order monochromatic aberrations on retinal image quality in a population of human eyes. *J Opt Soc Am A.* 2002;19:620-628.
44. Artal P, Navarro R. Monochromatic modulation transfer function for different pupil diameters: an analytical expression. *J Opt Soc Am A.* 1994;11:246-249.
45. Hofer H, Chen L, Yoon GY, Singer B, Yamauchi Y, Williams DR. Improvement in retinal image quality with dynamic correction of the eye's aberrations [abstract]. *Optics Express* [serial online]. 2001;8,:631-643. Available at: http://www.opticsexpress.org/oearchive/source/31887.htm. Accessed October 22, 2003.
46. Roorda A, Williams DR. The arrangement of the three cone classes in the living human eye. *Nature.* 1999;397:520-522.
47. Thibos LN, Bradley A, Still DL, Zhang X, Howarth PA. Theory and measurement of ocular chromatic aberration. *Vision Res.* 1990;30:33-49.
48. Campbell FW, Gubisch RW. The effect of chromatic aberration on visual acuity. *J Physiol.* 1967;192:345-358.
49. Yoon GY, Cox I, Williams DR. The visual benefit of the static correction of the monochromatic wave aberration. *Invest Ophthalmol Vis Sci.* 1999;40(Suppl):40.
50. Watson AB, Pelli DG. QUEST: A Bayesian adaptive psychometric method. *Perception & Psychophysics.* 1983;33:113-120.
51. Artal P, Hofer H, Williams DR, Aragon JL. Dynamics of ocular aberrations during accommodation. Paper presented at: Optical Society of America Annual Meeting; 1999.
52. Johnson CA. Effects of luminance and stimulus distance on accommodation and visual resolution. *J Opt Soc Am.* 1976;66:138-142.
53. Owsley C, Sekuler R, Siemsen D. Contrast sensitivity throughout adulthood. *Vision Res.* 1983;23:689-699.
54. Artal P, Ferro M, Miranda I, Navarro R. Effects of aging in retinal image quality. *J Opt Soc Am A.* 1993;10:1656-1662.
55. Guirao A, Gonzalez C, Redondo M, Geraghty E, Norrby S, Artal P. Average optical performance of the human eye as a function of age in a normal population. *Invest Optom Vis Sci.* 1999;40:203-213.
56. Cook CA, Koretz JF, Pfahnl A, Hyun J, Kaufman PL. Aging of the human crystalline lens and anterior segment. *Vision Res.* 1994;34:2945-2954.
57. Glasser A, Campbell MCW. Presbyopia and the optical changes in the human crystalline lens with age. *Vision Res.* 1998;38:209-229.
58. Oshika T, Klyce SD, Applegate RA, Howland HC. Changes in corneal wavefront aberrations with aging. *Invest Ophthalmol Vis Sci.* 1999;40:1351-1355.
59. Guirao A, Redondo M, Artal P. Optical aberrations of the human cornea as a function of age. *J Opt Soc Am A.* 2000;17:1697-1702.
60. Artal P, Berrio E, Guirao A, Piers P. Contribution of the cornea and internal surfaces to the change of ocular aberrations with age. *J Opt Soc Am A.* 2002;19:137-143.
61. Arnulf A, Dupuy O, Flamant F. Les microfluctuations d'accommodation de l'oiel et l'acuite visuelle pur les diametres pupillaires naturels. *CR Hebd Seanc Acad Sci Paris.* 1951;232:349-350.
62. Arnulf A, Dupuy O, Flamant F. Les microfluctuations de l'oiel et leur influence sur l'image retinienne. *CR Hebd Seanc Acad Sci Paris.* 1951;232:438-450.
63. Hofer H, Artal P, Singer B, Aragon JL, Williams DR. Dynamics of the eye's wave aberration. *J Opt Soc Am A.* 2001;18:497-506.
64. Guirao A, Williams DR, Cox IG. Effect of rotation and translation on the expected benefit of an ideal method to correct the eye's higher-order aberrations. *J Opt Soc Am A.* 2001;18:1003-1015.
65. Guirao A, Williams DR, Cox IG. Method for optimizing the benefit of correcting the eye's higher order aberrations in the presence of decentrations. *J Opt Soc Am A.* 2002;19:126-128.
66. Tomlinson A, Ridder III WH, Watanabe R. Blink-induced variations in visual performance with toric soft contact lenses. *Optom Vis Sci.* 1994;71:545-549.
67. Schwiegerling J, Snyder RW. Eye movement during laser in situ keratomileusis. *J Cataract Refract Surg.* 2000;26:345-351.
68. Guirao A, Williams DR, MacRae SM. Effect of beam size on the expected benefit of customized laser refractive surgery. *J Refract Surg.* 2003;19(1):15-23.
69. Oshika T, Klyce SD, Applegate RA, Howland HC, El Danasoury MA. Comparisons of corneal wavefront aberrations after photorefractive keratectomy and laser in situ keratomileusis. *Arch Ophthalmol.* 1999;127:1-7.
70. Thibos LN, Hong X. Clinical applications of the Shack-Hartmann aberrometer. *Optom Vis Sci.* 1999;76:817-825.

71. Williams DR, Yoon GY, Porter J, Guirao A, Hofer H, Cox I. Visual benefit of correcting higher order aberrations of the eye. *J Refract Surg*. 2000;16:S554-S559.

72. Applegate RA, Hilmantel G, Howland HC, Tu EY, Starck T, Zayac EJ. Corneal first surface optical aberrations and visual performance. *J Refract Surg*. 2000;16:507-514.